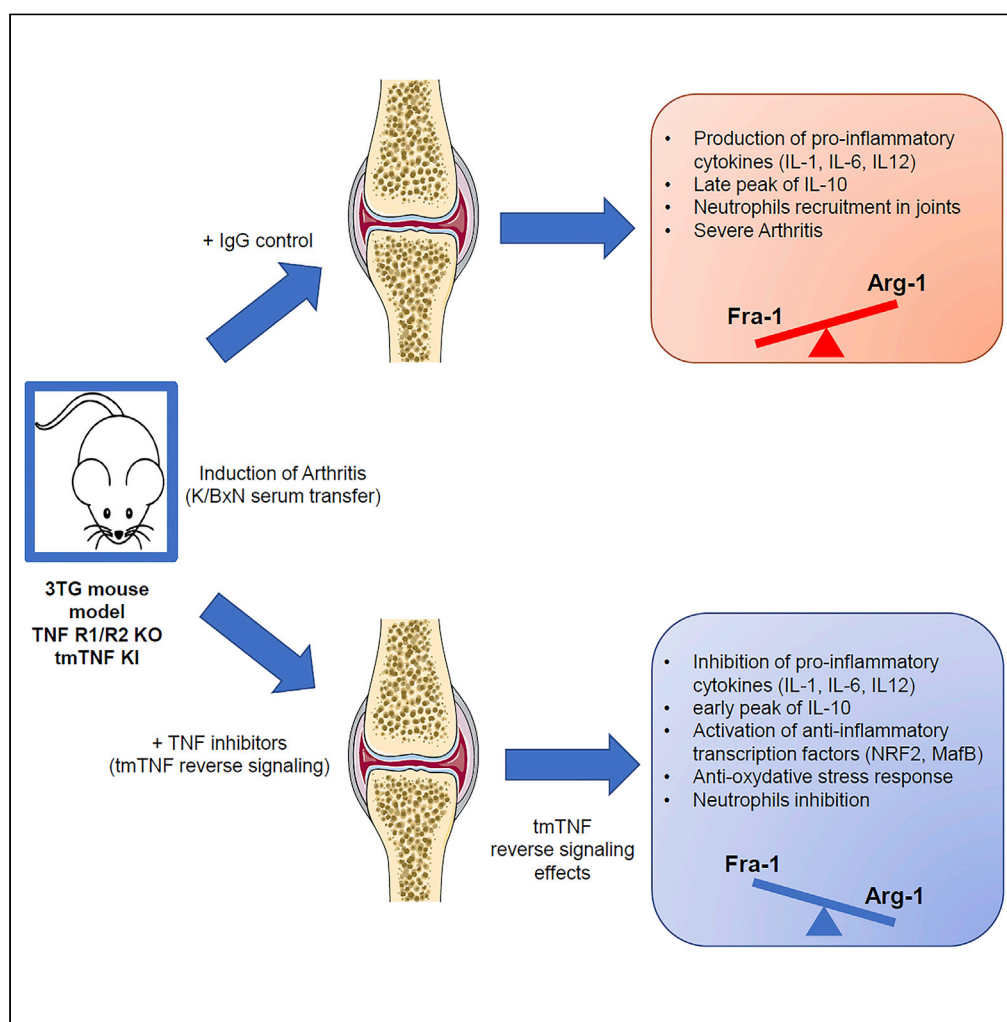


Article

Evidence for tmTNF reverse signaling *in vivo*:
Implications for an arginase-1-mediated
therapeutic effect of TNF inhibitors during
inflammation

Katy Diallo, Numa Simons, Souraya Sayegh, ..., Alain Cantagrel, Jean-Luc Davignon, Benjamin Rauwel

benjamin.rauwel@inserm.fr

Highlights

In vivo demonstration of tmTNF reverses signaling existence

tmTNF reverse signaling induces anti-oxidative stress response

tmTNF reverse signaling induces an arginase-1-mediated anti-inflammatory response

Reverse signaling is a complementary mechanism to TNF neutralization by anti-TNF

Article

Evidence for tmTNF reverse signaling *in vivo*: Implications for an arginase-1-mediated therapeutic effect of TNF inhibitors during inflammation

Katy Diallo,^{1,6} Numa Simons,^{1,2,6} Souraya Sayegh,¹ Michel Baron,¹ Yannick Degboé,^{1,2,3} Jean-Frédéric Boyer,² Andrey Kruglov,^{4,5} Sergei Nedospasov,⁵ Julien Novarino,¹ Meryem Aloulou,¹ Nicolas Fazilleau,¹ Arnaud Constantin,^{1,2,3} Alain Cantagrel,^{1,2,3} Jean-Luc Davignon,^{1,2} and Benjamin Rauwel^{1,7,*}

SUMMARY

In order to ascertain the significance of transmembrane tumor necrosis factor (tmTNF) reverse signaling *in vivo*, we generated a triple transgenic mouse model (3TG, TNFR1^{-/-}, TNFR2^{-/-}, and tmTNFKI/KI) in which all canonical tumor necrosis factor (TNF) signaling was abolished. In bone-marrow-derived macrophages harvested from these mice, various anti-TNF biologics induced the expression of genes characteristic of alternative macrophages and also inhibited the expression of pro-inflammatory cytokines mainly through the upregulation of arginase-1. Injections of TNF inhibitors during arthritis increased pro-resolutive markers in bone marrow precursors and joint cells leading to a decrease in arthritis score. These results demonstrate that the binding of anti-TNF biologics to tmTNF results in decreased arthritis severity. Collectively, our data provide evidence for the significance of tmTNF reverse signaling in the modulation of arthritis. They suggest a complementary interpretation of anti-TNF biologics effects in the treatment of inflammatory diseases and pave the way to studies focused on new arginase-1-dependent therapeutic targets.

INTRODUCTION

Tumor necrosis factor (TNF) is a homotrimeric pro-inflammatory and immunomodulatory cytokine. Like most members of the TNF superfamily, it exists either in a transmembrane form (transmembrane tumor necrosis factor [tmTNF]) or in a soluble form (soluble tumor necrosis factor [sTNF]) after cleavage of its precursor—(tmTNF)—by the protease TACE (TNF alpha converting enzyme, ADAM17). Both forms are bioactive (Moss et al., 1997; Zheng et al., 2004). Once secreted, sTNF acts in an autocrine or paracrine manner by binding to either one of its two receptors, TNFR1 and TNFR2 (Szondy and Pallai, 2017), which both also exist in transmembrane and soluble forms. TNFR1 is ubiquitously expressed on most cells and its stimulation leads to the activation of pro-inflammatory or apoptotic/necroptotic pathways depending on the context. TNFR2 is an inducible receptor whose expression is mostly restricted to immune, endothelial, and neuronal cells with a higher affinity for tmTNF (Grell et al., 1995). In addition to its pro-inflammatory role, TNFR2 could also act as an anti-inflammatory mediator and as such plays a role in cell signaling and promotes cell survival (Wajant et al., 2003).

Rheumatoid arthritis (RA) is a chronic inflammatory autoimmune disease that affects 0.5% of the adult population. It is characterized by the infiltration of synovial compartment of joints by immune cells (Smolen et al., 2016). Macrophages play a central role in the induction and maintenance of chronic inflammation during various stages of the disease (Siouti and Andreakos, 2019; Tak, 2000). One of the main mechanisms involved in this process is the secretion of pro-inflammatory cytokines such as interleukin (IL)-1 β , IL-6, and TNF. The latter plays a leading role in the activation of immune responses through the production of inflammatory mediators but also by stimulating osteoclastogenesis (Butler et al., 1995; Haworth et al., 1991; Kitzura, 2005).

The development of TNF inhibitors has permitted to control the activity of RA in a substantial proportion of patients (Feldmann et al., 2010). There are currently five different molecules available, two human anti-TNF

¹INFINITY, Toulouse Institute for Infectious and Inflammatory Diseases, INSERM U1291, CNRS U5051, University Toulouse III, Toulouse, France

²Centre de Rhumatologie, CHU de Toulouse, Toulouse, France

³Faculté de Médecine, Université Paul Sabatier Toulouse III, Toulouse, France

⁴German Rheumatism Research Center (DRFZ), a Leibniz Institute Berlin 10117, Germany

⁵Engelhardt Institute of Molecular Biology, Russian Academy of Sciences, Moscow 119991, Russia

⁶These authors contributed equally

⁷Lead contact

*Correspondence:

benjamin.rauwel@inserm.fr

<https://doi.org/10.1016/j.isci.2021.102331>



monoclonal antibodies (adalimumab, golimumab), a pegylated antigen-binding fraction of humanized antibodies (certolizumab pegol), a murine chimeric antibody (infliximab), and a soluble form of TNFR2 coupled to human Fc domain (etanercept [ETA]) (Taylor and Feldmann, 2009).

Unfortunately, these treatments are not always effective, with an estimated 40% of unsatisfactory responses to one of these biologics. TNF antagonists are thought to control inflammation by preventing the binding of sTNF to its receptors and are all equally effective in lowering TNF concentrations (Kaymakcalan et al., 2009; Mitoma et al., 2018; Nesbitt et al., 2007). However, they are also all able to bind tmTNF (Horiuchi et al., 2010). It has been demonstrated that tmTNF can act *in vitro* as a signaling receptor through a mechanism known as “reverse signaling” (Eissner et al., 2000) which may play a role in cellular communications (Eissner et al., 2004).

Specifically, TNFR2 was shown to interact with tmTNF and induce intra-cellular responses through reverse signaling that contributes to an increased lipopolysaccharides (LPS) resistance, via the activation of the mitogen-activated protein kinase/extracellular signal-regulated kinase pathway (Boyer et al., 2007; Eissner et al., 2000; Kirchner et al., 2004; Mitoma et al., 2005; Pallai et al., 2016). Furthermore, the involvement of nuclear factor erythroid-2-related factor 2 (Nrf2) activation during reverse signaling was recently discovered in our laboratory (Boyer et al., 2016). More recently, internalization of anti-TNF antibody/tmTNF complexes by dendritic cells has been demonstrated. The authors have explored anti-drug-antibody genesis but other consequences of such internalization, including reverse signalization, can be also envisioned (Deora et al., 2017).

Several studies implicated a role for reverse signaling in various biological processes including *in vitro* neuronal growth (Kisiswa et al., 2013), macrophage inflammation (Meusch et al., 2009), and apoptosis (Meusch et al., 2013). However, the significance of tmTNF reverse signaling *in vivo* has yet to be demonstrated.

The K/BxN model induces peripheral arthritis phenotypically similar to RA in mice (Korganow et al., 1999; Kouskoff et al., 1996). Mice injected with K/BxN serum develop peripheral arthritis, which relies solely on innate immunity (macrophages, polynuclear neutrophils, complement) and more specifically on neutrophils (Ji et al., 2002a; Wipke and Allen, 2001), is partially dependent on TNF (Ji et al., 2002b), and resolves within 14–21 days.

No model was available to define TNF reverse signaling *in vivo* and to study the impact of tmTNF reverse signaling on macrophage polarization and inflammation.

To this end, we generated a triple transgenic mouse model (3TG) lacking TNFR1 and TNFR2 expression (TNFR1/R2 KO) and expressing TNF at a physiological level exclusively in its transmembrane form (tmTNF KI) due to knock-in mutations (Ruuls et al., 2001). These 3TG mice were developed as an experimental model to simplify the study of tmTNF reverse signaling *in vitro* but also *in vivo*. The comparison with wild type (WT) animals is not the aim of this study and will be discussed later. In primary bone-marrow-derived macrophages (BMDMs) from these mice, we evaluated the effects of anti-TNF stimulation on macrophage polarization *in vitro*. We observed that tmTNF reverse signaling induced a decrease of the pro-inflammatory transcription factor Fra-1 and consequently an upregulation in pro-resolutive transcription factors and effectors such as arginase-1 (Arg-1). Furthermore, we observed that tmTNF reverse signaling induced an early peak of IL-10 and inhibited pro-inflammatory cytokines, such as IL-6 and IL-12. Finally, using the K/BxN serum injection arthritis model in WT and 3TG mice, we showed that anti-TNF injections induced an increase in pro-resolutive transcription factor and enzyme (Arg-1) in bone marrow precursors and inhibited arthritis. Furthermore, pro-inflammatory IL-1 β was inhibited, and neutrophils were less numerous in the joints of treated mice, thus demonstrating for the first time the significance of reverse signaling *in vivo* and implicating a novel interpretation of the effects of anti-TNF therapy in the treatment of inflammatory diseases, such as RA.

RESULTS

Internalization of soluble TNF receptor 2 (ETA) through its interaction with tmTNF suggests reverse signaling in macrophages

We first validated our mouse model specifically developed to study reverse signaling. By flow cytometric analysis of immune cell populations in the spleen and inguinal lymph nodes, we did not observe significant

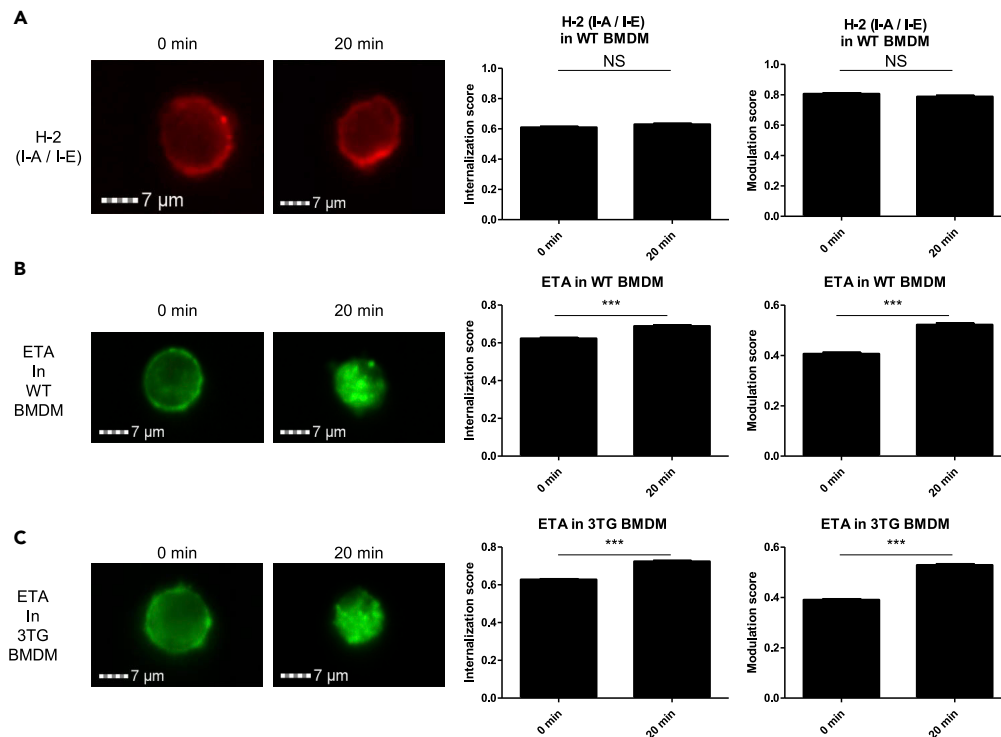


Figure 1. Internalization of soluble TNF receptor 2 (ETA) through its interaction with tmTNF suggests reverse signaling in macrophages

Non-polarized BMDMs were stimulated with LPS (50ng/mL) 30 min prior to staining in presence of Fc blocker with H-2-PE-Cy5 in WT (A) or ETA-dyeLight488 in WT (B) and 3TG (C) during 20 min at 4° (0 min) or 37°C (20min). Internalization and modulation scores were analyzed by imaging cytometry (ISX). Data are presented as mean \pm SEM of internalization or modulation scores (***) $p < 0.001$, $n > 500$ events, Student's t test). Images are representative of 3 independent experiments with more than 500 events analyzed each time.

differences in these cell populations between WT and 3TG mice (Figures S1A–S1C). As expected, secretion of TNF was null in 3TG mice (Figure S1D). The expression of tmTNF before and after stimulation with LPS + IFN- γ was similar in BMDMs from WT and 3TG mice, suggesting an equivalent capacity to interact with its ligands (Figure S1E).

We then investigated the interaction of soluble TNF receptor 2 (ETA) with tmTNF in BMDMs from 3TG mice. To this end, we performed imaging cytometry on BMDMs after 30 min of stimulation with LPS (50 ng/mL) as a mean to increase tmTNF cell surface expression. Cells were then incubated with ETA conjugated to DyeLight488 (ETA-488), and an internalization assay was performed. As a control, we used anti-H-2 (I-A/I-E) phycoerythrin-conjugated antibody which did not induce any internalization (Figure 1A). Higher internalization and modulation score at 20 min indicate that ETA-488 was internalized in WT (Figure 1B) as well as in 3TG BMDMs (Figure 1C). This internalization was observed in the presence of an Fc-blocker suggesting that it was mediated by interaction with tmTNF and not through Fc receptor. Furthermore, higher internalization was observed in 3TG in comparison with WT (0.68 vs 0.73, $p < 0.001$), suggesting that in the absence of sTNF, enhanced interaction of ETA-488 with tmTNF was detected. Similar results were obtained with rat anti-murine-TNF antibody (MP6-XT22) in WT and 3TG cells (Figures S2A and S2B). These results demonstrated an internalization of soluble TNF receptor 2 (ETA) and suggested as a consequence of tmTNF/anti-TNF interaction, an ETA-mediated reverse signaling in macrophages as observed in our laboratory with certolizumab pegol (Boyer et al., 2016).

Impact of tmTNF reverse signaling on macrophage polarization *in vitro*

TNF inhibitors are known to modulate macrophage polarization (Degboé et al., 2019). We thus assessed the effects of tmTNF reverse signaling on macrophage phenotypes. BMDMs were harvested from WT

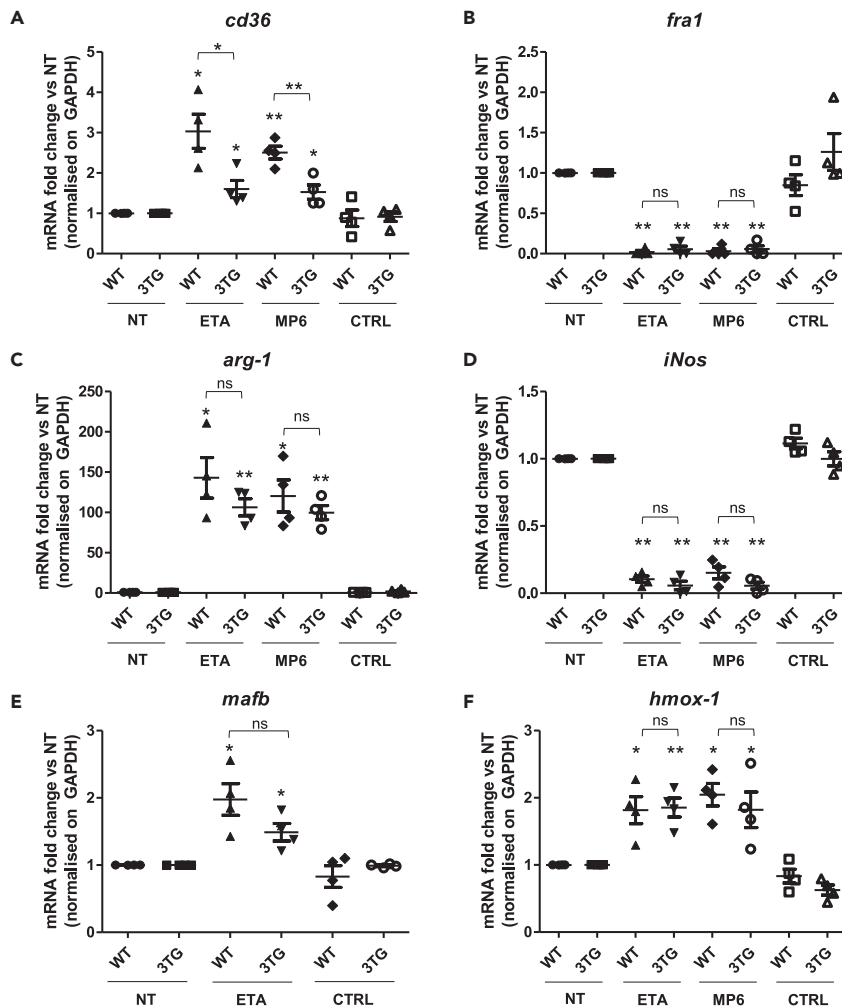


Figure 2. tmTNF reverse signaling phenotypic impact on macrophage polarization in vitro

WT or 3TG BMDMs were obtained after 7 days of differentiation with recombinant M-CSF (50 ng/mL) in the presence or absence (NT) of 10 μ g/mL of TNF soluble receptor (ETA), anti-TNF antibody (MP6-XT22), or IgG control (CTRL). BMDMs were then polarized into pro-inflammatory M1 macrophage during 24 hr with LPS (100 ng/mL) and IFN- γ (25 ng/mL) in the presence or not (NT) of fresh ETA, MP6-XT22, or CTRL.

RNA were extracted and *cd36* (A), *fra-1* (B), *arg1* (C), *iNos* (D), *mafb* (E), and *hmox-1* (F) mRNA expression was analyzed by RT-qPCR in 3TG and WT BMDMs. Data are presented as mean \pm SEM of mRNA fold change vs NT normalized on *gapdh*. (n = 4, ns p > 0.05, *p < 0.05, **p < 0.01, Mann-Whitney U test performed).

and 3TG mice and cultured with or without a control IgG (CTRL), an anti-murine-TNF antibody (MP6-XT22) or a soluble TNF-R2 (ETA) during their differentiation. After 7 days, BMDMs were polarized into a pro-inflammatory phenotype by adding LPS/IFN- γ for 24 hr. Using flow cytometry analysis, we observed that anti-TNF antibody but not ETA inhibited the expression of a panel of pro-inflammatory markers during BMDM differentiation and M1 polarization. Indeed, MP6-XT22 treatment led to a decrease of Ly6C and CD40 expression in WT cells. However, this inhibition was not observed in 3TG cells, suggesting that this effect was not mediated by reverse signaling (Figure S3A–S3C). No difference was observed in CD80, GPR18, CD38, and FPR2 expression levels in anti-TNF-treated WT and 3TG BMDMs (Figures S3D–S3G). When we focused on the pro-resolutive markers CD163 and CD206, no modulation was detected between cells obtained from WT or 3TG mice treated with anti-TNF and those that were not treated (Figure S3H and S3I). No effect was observed in presence of rat control IgG (Figure S4)

Then, we analyzed the expression of the scavenger receptor CD36 which was previously shown to be up-regulated by anti-TNF treatment in human monocytes (Boyer et al., 2007). In our BMDM model, we

observed a significant increase of the CD36 surface (Figure S5A) and mRNA expression (Figure 2A) in WT as well as in 3TG cells, suggesting that it was mediated by reverse signaling. These results demonstrated that only anti-TNF antibodies inhibit the expression of pro-inflammatory markers Ly6C and CD40 but both antibodies and ETA promote pro-resolutive marker CD36. However, tmTNF reverse signaling was only involved in the modulation of CD36 expression.

We next sought to evaluate the impact of tmTNF reverse signaling on the expression of functional effectors of pro-inflammatory and pro-resolutive macrophages. The pro-inflammatory effects of Fra-1 are controlled through the balance of Fra-1/Arg-1 (Hannemann et al., 2019). *In vitro*, we observed a strong decrease in Fra-1 expression in WT and 3TG M1 macrophages in the presence of anti-TNF but not in the IgG control-treated cells (Figure 2B). Consistent with Fra-1 decrease, a strong increase of Arg-1 mRNA and protein was confirmed in anti-TNF treated cells (Figures 2C and S5B), thus reversing the balance of Fra-1/Arg-1 (Figure S5C). Furthermore, expression of the pro-inflammatory enzyme Nos2, also involved in the L-arginine pathway, was inhibited by anti-TNF in comparison with the IgG control (Figure 2D). These observations lead to the analysis of MafB, a pro-regulator of Arg-1 and anti-inflammatory transcription factor in macrophages (Kim, 2017). We demonstrated that MafB mRNA was increased after stimulation by TNF soluble receptor in WT and 3TG BMDMs (Figure 2E), and this correlated with an increase of MafB protein in the anti-TNF stimulated BMDMs (Figure S5D), consistent with the upregulation of Arg-1 and anti-inflammatory macrophage polarization. We could also detect an upregulation of the transcription factor C-myc (Figure S5E), although this upregulation was not significant in WT BMDMs. No significant differences were observed in regard to the pro-resolutive transcription factors Mrc-1 and Egr-2 (Figures S5F and S5G).

We also recorded an upregulation of the anti-oxidative stress response genes, *hmx-1* (Figure 2F) and *gclc* (Figure S5H). These effectors are under the control of the anti-inflammatory NRF2 which we had previously linked to reverse signaling in human monocytes (Boyer et al., 2016). No effect was observed in presence of rat IgG control (Figure S5I). All these modulations in favor of pro-resolutive effectors were detected with similar intensity in WT and 3TG BMDMs, except for *cd36* where the upregulation is higher in WT. These results indicate that tmTNF reverse signaling may impact macrophage polarization in favor of pro-resolutive functions.

tmTNF reverse signaling induces an early peak of IL-10 secretion and inhibits pro-inflammatory cytokines *in vitro*

To investigate the consequences of tmTNF reverse signaling-mediated upregulation of pro-resolutive effectors, cytokine production was measured during LPS/IFN γ -mediated M1 polarization in the presence of TNF inhibitors. When control Ab were used, production of IL-10 in cells from WT mice increased over a 24 hr time period, which reflected the negative feedback of TNF-induced inflammation (Sabat et al., 2010) (Figure 3A). In contrast, in cells from 3TG mice, production of IL-10 was modest, due to the absence of TNF-induced negative feedback (Figure 3B). Treatment with anti-TNF and ETA decreased the production of IL-10 in WT cells at the 24th hour and in 3TG cells at the 16th hour of culture. Confirming our observations in human macrophages (Degboé et al., 2019), TNF inhibitors induced an early peak of IL-10 secretion in WT (Figure 3A) and 3TG (Figure 3B) after 6 hr of stimulation. As no TNF receptors are present in 3TG mice, this early production of IL-10 is likely to result from tmTNF reverse signaling. Consistent with this early peak of IL-10 secretion, we observed a strong decrease in IL-6 (Figure 3C) and IL-12p70 (Figure 3D) in anti-TNF-treated cells compared to controls. IL-1 β and TGF- β were not detectable in cell supernatants. These results indicate that tmTNF reverse signaling induces a rapid upregulation of IL-10 secretion coupled to an inhibition of IL-6 and IL-12 production.

tmTNF reverse signaling anti-inflammatory effect is mainly mediated by arginase-1

To analyze the impact of tmTNF reverse signaling-mediated arginase-1 upregulation on pro-inflammatory cytokine inhibition, we used CB-1158, a specific arginase inhibitor which has been shown to block myeloid cell-mediated immune suppression (Steggerda et al., 2017). BMDMs were treated with CB-1158 during differentiation and polarization with or without ETA or control IgG. We observed that *cd36* upregulation was not significantly modulated by the inhibition of Arg-1 (Figure 4A) in contrary to *hmx-1* upregulation observed with ETA treatment which was inhibited in the presence of Arg-1 inhibitor (Figure 4B). When we focused on pro-inflammatory cytokines, we revealed that ETA-mediated downregulation of *il-1 β* , *il-6*, and *il-12* was less efficient when Arg-1 was inhibited (Figures 4C–4E). Finally, we observed that *il-10* upregulation by anti-TNF was also inhibited in the presence of CB-1158. All these modulations were observed

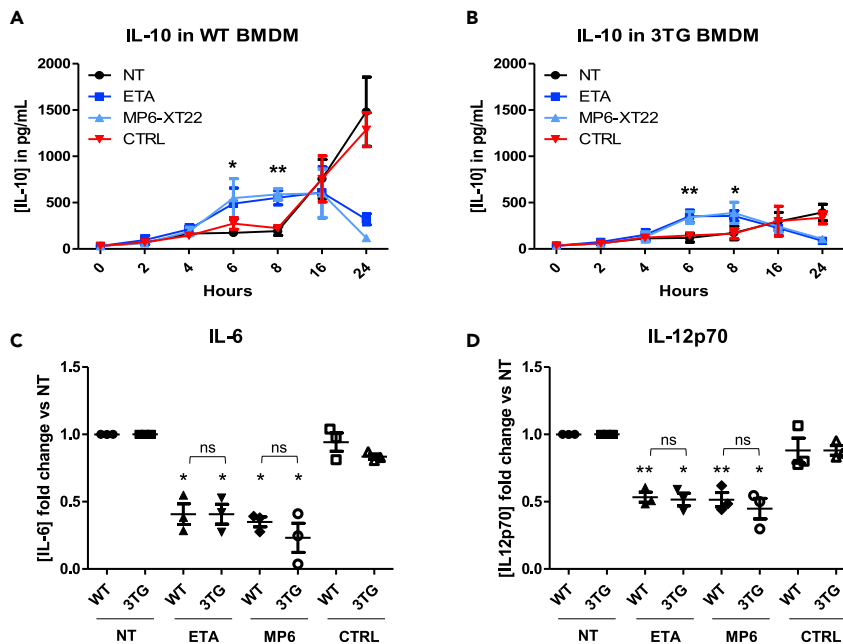


Figure 3. tmTNF reverse signaling induces an early peak of IL-10 secretion and inhibits pro-inflammatory cytokines *in vitro*

WT or 3TG BMDMs were obtained during 7 days of differentiation with recombinant M-CSF (50 ng/mL) in presence or absence (NT) of TNF soluble receptor (ETA), anti-TNF antibody (MP6-XT22), or IgG control (CTRL) prior to being polarized into pro-inflammatory M1 macrophage during 24 hr with LPS (100 ng/mL) and IFN- γ (25 ng/mL) in presence or not (NT) with fresh ETA, MP6-XT22, or CTRL.

Twenty-four hour secretion kinetic of IL-10 in M1 polarized in WT(A) and 3TG (B) BMDM was analyzed by ELISA. IL-10 concentration at 6 hr and 10 hr after stimulation by LPS-IFN- γ is represented in histograms. After 24 hr of M1 polarization, IL-6 (C) and IL12p70 (D) concentrations were analyzed by cytometric bead array. Data represent mean \pm SEM of cytokine concentration fold change versus NT (n = 3, *p < 0.05, **p < 0.01, Mann-Whitney U test). ELISA, enzyme-linked immunosorbent assay.

with similar intensity in WT and 3TG BMDMs. These results suggested that tmTNF reverse anti-inflammatory effect is mainly mediated by the upregulation of Arg-1.

tmTNF reverse signaling role in the therapeutic response to TNF inhibitors during arthritis

Finally, we studied the role of tmTNF reverse signaling in the therapeutic response to anti-TNF therapy during arthritis. Eight-week-old 3TG or WT mice were pre-injected with either anti-TNF or control IgG 5 and 3 days prior to inducing K/BxN serum transfer arthritis as described in our experimental protocol (Figure S6A). At day 0, bone marrow precursor cells from femurs and tibias were collected, and the expression of pro-inflammatory and pro-resolutive markers was analyzed by reverse transcription quantitative polymerase chain reaction (RT-qPCR). Injection of anti-TNF or ETA upregulated the expression of pro-resolutive effectors Arg-1, Mrc-1, and Egr-2 in precursor cells *in vivo* in WT as well as in 3TG cells (Figures 5A, 5B, S6B, and S6C). Fra-1 mRNA was not detectable in those precursor cells, and no significant differences for c-myc and CD38 expression were observed (Figures S6B and S6C). These results argue in favor of tmTNF reverse signaling *in vivo* and its impact on pro-resolutive effector expression. At day 0 and 2, mice were intraperitoneally injected with K/BxN serum to induce arthritis. Animals received control IgG or anti-TNF injection at day 0, 2, 4, 7, 9, and 11. Evolution of arthritis was evaluated over 14 days. We observed that ETA injection in WT mice decreased the arthritis score over the course of the experiment (p < 0.001, two-way analysis of variance [ANOVA] test) (Figure 5C). Although the severity of arthritis was lower, inhibition of arthritis was also observed in 3TG mice (Figure 5D) (p < 0.001, two-way ANOVA test), demonstrating that this effect was indeed due to tmTNF-mediated reverse signaling, which was confirmed using an anti-TNF antibody (MP6-XT22). This antibody significantly lowered the clinical score in WT as well as in 3TG mice (Figure 5D). There was no significant effect of control IgG injection on the arthritis cumulative score (Figures

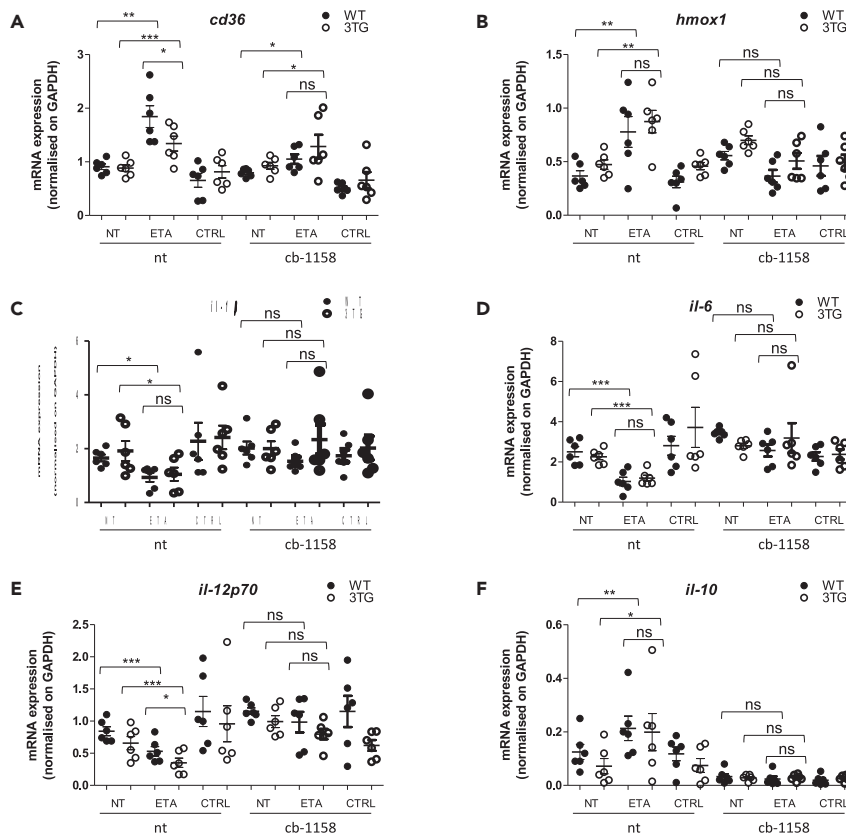


Figure 4. tmTNF reverse signaling anti-inflammatory effect is mainly mediated by ARG-1

WT or 3TG BMDMs were obtained during 7 days of differentiation with recombinant M-CSF (50 ng/mL) in presence or absence (NT) of TNF soluble receptor (ETA), anti-TNF antibody (MP6-XT22) or IgG control (CTRL), and arginase inhibitor (CB-1158; 10 μ M) prior to being polarized into pro-inflammatory M1 macrophage during 24 hr with LPS (100 ng/mL) and IFN- γ (25 ng/mL) in presence or not (NT) with fresh ETA, MP6-XT22 or CTRL, and CB-1158. RNAs were extracted and *cd36* (A), *hmox-1* (B), *il-1 β* (C), *il-6* (D), *il-12p70* (E), and *il-10* (F) mRNA expression was analyzed by RT-qPCR in 3TG and WT BMDMs. Data are presented as mean \pm SEM of mRNA fold change vs NT normalized on *gapdh*. (n = 6, *p < 0.05, **p < 0.01, ***p < 0.001, unpaired t test performed).

S7A and S7B), further proving that the effects of anti-TNF injection were due to tmTNF reverse signaling and were not mediated by Fc-receptors. Cytokine concentrations were measured in blood samples at the peak of arthritis (day 7). As expected, in contrary of WT mice, no sTNF was detected in 3TG mice (Figure S7C). Nevertheless, we recorded a significant decrease in IL-6 and a trend toward a decrease of IL-12 in 3TG mice (Figure 5E). IL-1 β was not detectable in sera. IL-10 increased after anti-TNF treatment but was statistically significant only with ETA (Figure 5E). This lack of significance was probably due to a lower impact of anti-TNF in peripheral blood than in arthritis. To focus on the effect of reverse signaling in joints, mice treated or not with ETA or IgG1 control were sacrificed at the peak of arthritis (Figure 6A). By flow cytometry analysis of joint cell populations, we could observe that anti-TNF treatment did not have any significant impact on total monocytes, even if a trend toward an upregulation of pro-resolutive Ly6c^{low} Cd11b⁺ monocytes was recorded in WT ETA-treated mice as observed in BMDMs *in vitro* (Figure 6B). No effect on dendritic cells (Figures 6C) and B lymphocytes (Figure S7D) was noted. We observed an increase in macrophages only in treated WT mice (Figure 6D), suggesting that this effect is principally due to sTNF neutralization. Nevertheless, the principal effectors in K/BxN serum transfer arthritis model, neutrophils (Wipke and Allen, 2001), were decreased in both WT and 3TG ETA-treated mice joints (Figure 6E). These results demonstrate the anti-inflammatory effect of reverse signaling, strengthened by the observed upregulation of Arg-1 and IL-10 mRNA coupled with the downregulation of pro-inflammatory Fra-1 and IL-1 β expression in WT as in 3TG joints (Figure 6F), although no significant effect was observed on IL-6 and IL-12 mRNA

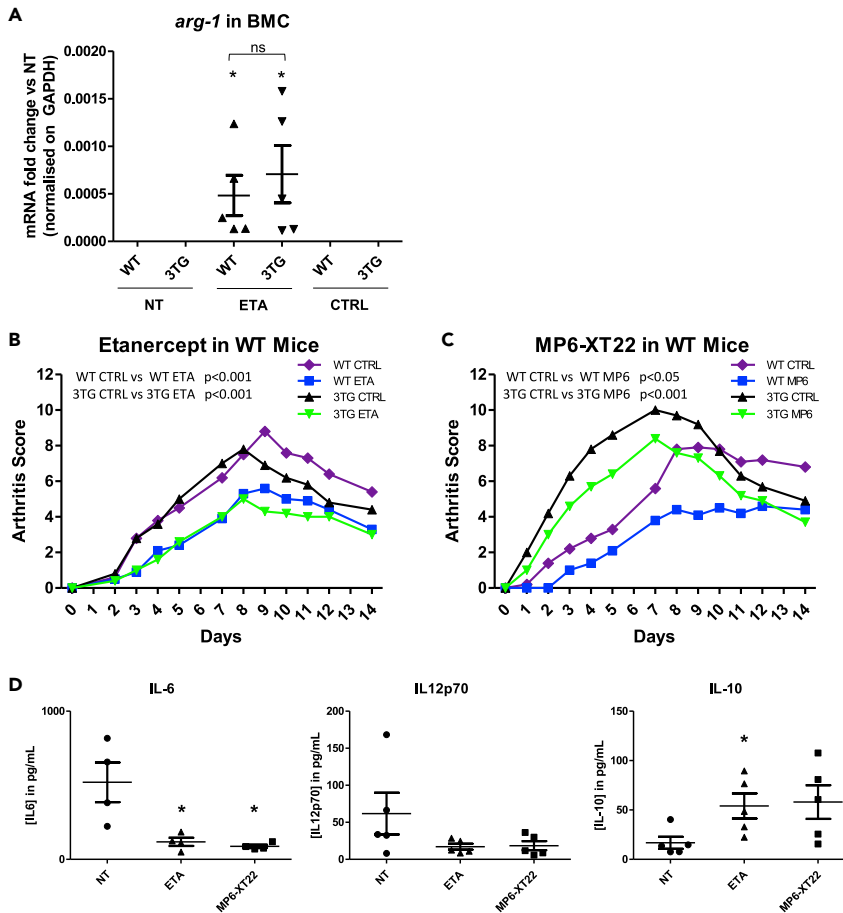


Figure 5. tmTNF reverse signaling role in the therapeutic response to TNF inhibitors during arthritis

Arthritis was induced by K/BxN serum transfer in 3TG or WT mice treated or not with anti-TNF (ETA or MP6-XT22) or control IgG1 (CTRL).

(A) At day 0, the bone marrow from 4 WT or 3TG mice of each group (NT, ETA, and CTRL) was collected and mRNA from precursor cells was extracted. Expression of *Arg-1* was analyzed by RT-qPCR. Data represent mean \pm SEM of mRNA expression normalized on *gapdh* expression (n = 4). Statistics analysis was performed with Mann-Whitney U test. ND = non detectable.

(B and C) Clinical effect of (B) TNF soluble receptor 2 (etanercept, ETA, 10 mg/kg) or (C) anti-mouse TNF rat antibody (MP6-XT22, 10 mg/kg) on the development of arthritis (arthritic score) in the WT or 3TG K/BxN serum-transferred mice (n = 5 per group). Control (CTRL): untreated K/BxN serum-transferred mice. Results are presented as mean arthritic score during 14 days after K/BxN injection. Data represent mean \pm SEM. p value for arthritis score was calculated by repeated measurements of two-way ANOVA tests.

(D) Concentrations of IL-6, IL-12p70, and IL-10 in blood samples of 3TG arthritic mice were quantified by cytometric bead array 7 days after K/BxN first injection. Data represent mean \pm SEM of cytokine concentrations (n = 5, except for IL-6, n = 4). *p < 0.05 as calculated with Mann-Whitney U test).

expression (Figures S7E and S7F). Thus, our experiments strongly support an anti-inflammatory role for reverse signaling *in vivo* and its implications in the therapeutic response to anti-TNF during arthritis.

DISCUSSION

In this work, we present evidence for *in vivo* anti-TNF-induced tmTNF reverse signaling and demonstrate for the first time its impact on macrophage polarization and its functional role in the clinical response to TNF blocking therapy during arthritis *in vivo*.

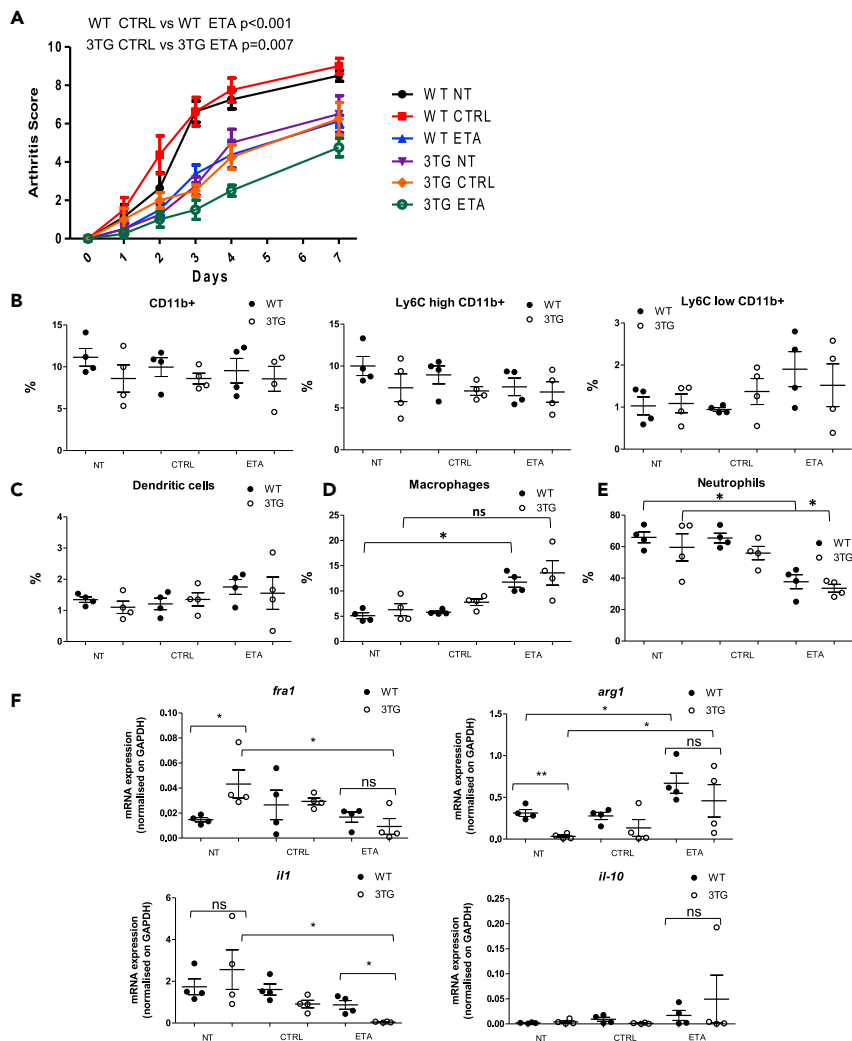


Figure 6. tmTNF reverse signaling impact on immune cells and inflammation in arthritic joints

Eight-week-old 3TG or WT mice were injected at days 0 and 2 intraperitoneally with 200 μ L of 60-week-old K/BxN mice serum to induce arthritis. Mice were injected with 10 mg/kg of anti-TNF (ETA) or control IgG1 (CTRL) 5 and 3 days prior to inducing arthritis with the first injection of K/BxN serum and at days 0, 2, 4, and 7. Mice were sacrificed at day 7, and joints were dissected.

(A) Clinical effect of ETA or CTRL on the development of arthritis (arthritic score) in the WT (left panel) or 3TG (right panel) K/BxN serum-transferred mice ($n = 4$ per group). Control (CTRL): untreated K/BxN serum-transferred mice. Results are presented as mean arthritic score during 7 days after K/BxN injection. Data represent mean \pm SEM. p value for arthritis score was calculated by repeated measurements of two-way ANOVA tests.

(B–E) Flow cytometry analysis of percentage of monocytes (B), dendritic cells (C), macrophages (D), and neutrophils (E) in joints.

(F) RT-qPCR analysis of *Fra-1*, *Arg-1*, *IL-1 β* , and *IL-10* mRNA expression. Data represent mean \pm SEM of percentage of leaving cells or mRNA expression normalized on GAPDH ($n = 4$, ns $p > 0.05$, $*p < 0.05$ as calculated with Mann-Whitney U test).

Contrary to what was previously published (Nguyen et al., 2018), we observed that ETA binds to tmTNF and can be internalized by macrophages. This observation suggests that ETA as well as anti-TNF antibody is capable of inducing a reverse signaling through tmTNF. We could hypothesize that this internalization will induce an increase of reactive oxygen species which be responsible of NRF2 activation as previously described (Boyer et al., 2016) or will induce an outside-to-inside signaling similar or different of the previously described for anti-TNF antibodies (Mitoma et al., 2005). Studying the complete mechanism of reverse signaling is a story in itself and will be the subject of future work.

In vitro, we saw that TNF blockade during WT macrophage differentiation, by antibodies but not ETA, inhibited the expression of pro-inflammatory surface markers, such as CD40 and Ly6c. Such inhibition can be attributed to the neutralization of sTNF as it was not observed in our 3TG model. This difference between antibody and ETA may be due to a different interaction with sTNF and tmTNF (Kohno et al., 2007; Scallon et al., 2002). As opposed to human macrophage polarization by TNF inhibitors (Degboé et al., 2019), we did not see any modulation of CD163 and CD206 in murine macrophages. Those effects might be specific to human macrophages or might be due to the source of cells used (blood vs bone marrow). However, in 3TG as well as in WT BMDM, we observed an increase in the expression of scavenger receptor CD36- and NRF2-dependent anti-oxidative stress response genes, thus proving and confirming that CD36 modulation and NRF2 activation in response to anti-TNF is due to tmTNF-mediated reverse signaling (Boyer et al., 2016).

From a functional point of view, by studying the transcription factors in addition to the key enzymes of the induction/maintenance or the resolution of inflammation, we concluded that tmTNF reverse signaling induced a pro-resolutive switch to the detriment of certain pro-inflammatory actors. Indeed, we observed in our 3TG model as in WT BMDMs that the reverse signaling inhibited the expression of the transcription factor Fra-1 and increased the pro-resolutive enzyme Arg-1 expression. Recently, it has been shown that this Fra-1/Arg-1 balance is related to the severity of RA (Hannemann et al., 2019). It has already been described that soluble TNF neutralization could increase Arg-1 and pro-resolutive macrophage differentiation (Kroner et al., 2014; Kratochvill et al., 2015; Atretkhany et al., 2016; Schleicher et al., 2016). Nevertheless, with the help of our 3TG model, we demonstrated for the first time that tmTNF reverse signaling is also able to do it. This suggests that there is a complementary effect of reverse signaling and soluble cytokine neutralization that could explain the significant differences between WT and 3TG animals. Indeed, TNF blocker effects were always more efficient in WT animals, due to the combination of sTNF neutralization and tmTNF reverse signaling. More interestingly, we noticed that this upregulation of Arg-1 is correlated with the increase of mRNA and nuclear protein expression of MafB, a positive regulator of Arg-1 which is able to bind to its promoter and regulate a pro-resolutive polarization of macrophages (Kim, 2017). We also evidenced that the inhibition of pro-inflammatory cytokines and anti-oxidative stress response of tmTNF reverse signaling is principally mediated by this upregulation of Arg-1. In addition, we observed an increase in pro-resolving transcription factors such as c-myc, MRC-1, or Egr2 as well as an inhibition of the M1 Nos2 enzyme.

As for cytokine secretion, an early peak of IL-10 was noticed, similar to human macrophages cultured in the presence of TNF inhibitors (Degboé et al., 2019). This IL-10 early peak is then followed by an inhibition of pro-inflammatory cytokine production. As previously described in Degboé's work, anti-inflammatory effects and pro-resolutive macrophage differentiation of TNF blockers are more efficient when they are added during all the differentiation and polarization time (data not shown) in contrary of polarization alone. This suggests that the TNF blocker effects in patients are not only immediate but also over time. Thus, our data provide conclusive evidence that TNF targeting is able, through tmTNF reverse signaling, to inhibit the secretion of pro-inflammatory cytokines.

Furthermore, in line with the anti-inflammatory effect observed *in vitro*, we demonstrated that tmTNF reverse signaling inhibits arthritis *in vivo*. The low TNF dependence of K/BxN serum transfer models has allowed us to induce arthritis in our 3TG model. Injection of anti-TNF during K/BxN serum-induced arthritis decreased clinical score in WT as in 3TG mice, suggesting a crucial role of tmTNF reverse signaling in the therapeutic response to anti-TNF biologics. We had to use 2 pre-injections of ETA or MP6-XT22 as it has been described that ETA does not have an impact in WT mice in K/BxN serum transfer models without pre-injection (Victoratos and Kollias, 2009), certainly due to the fast kinetic of this model. Although we used a prophylactic treatment model, the interest of our study is focused on the demonstration of the existence of tmTNF reverse signaling *in vivo* and its crucial role in the anti-inflammatory effect of anti-TNF agents. Since patients have constant circulating anti-TNF levels during treatment, it is also conceivable that this prophylactic effect may be found in cells which are differentiating during the disease. To better understand the consequences of tmTNF reverse signaling in arthritis, we focused on joint cell populations and discovered that anti-TNF treatment decreased localized inflammation. Indeed, in anti-TNF treated WT and 3TG joints, neutrophil population was inhibited and this was accompanied by a decrease of pro-inflammatory IL-1 β expression. This inhibition of neutrophils could be due to direct tmTNF reverse signaling as they express TNF and logically tmTNF or due to the neutralization of TNF that could not induce pro-survival signals in these cells (Cowburn et al., 2004; Wright et al.,

2011). Furthermore, increases of pro-resolutive effectors (IL-10 and ARG-1) were also observed, strengthening the anti-inflammatory effect of tmTNF reverse signaling.

The demonstration that anti-TNF agents can ameliorate arthritis by their action on tmTNF leads to a new interpretation of the effects of anti-TNF therapy in RA and other inflammatory diseases. We discovered novel mechanisms of action of these drugs, including the activation of MafB and NRF2 transcription factors and the increase of the anti-inflammatory regulator IL-10 and Arg-1. We can hypothesize that the intra-individual variability in anti-TNF clinical responses depends in part on the proteins recruited during the formation and internalization of the tmTNF/anti-TNF complexes (Deora et al., 2017; Ogura et al., 2016) and may be linked to specific epitopes recognized by the anti-TNF biologics used. Setting apart the roles of tmTNF reverse signaling on the one hand and the inhibition of sTNF on the other hand will help to better understand the mechanisms of action of TNF inhibitors.

Finally, this 3TG model permits us to highlight the effect of tmTNF reverse signaling on inflammation and oxidative stress response in the absence of TNFR1/R2 expression and a mutated tmTNF (deletion/mutation combination) with normal cell-surface expression and function which avoid an interaction with other receptors (Decoster et al., 1995). Nevertheless, we observed a more important effect in WT animals and cells in comparison with 3TG ones. This fact is certainly due to the combined effect of soluble TNF neutralization and tmTNF reverse signaling. This leads to the interpretation that tmTNF reverse signaling is not the principal or the only mechanism of TNF blockers but a complementary mechanism to soluble TNF neutralization. As tmTNF cell surface expression and signalization have been described to be related to an efficient clinical response to TNF blockers (Kadijani et al., 2017; Meusch et al., 2015), we could hypothesize that this reverse signaling is an essential complementary effect for therapeutical response.

In conclusion, our data provide evidence for the involvement of tmTNF reverse signaling in the anti-TNF-mediated modulation of arthritis *in vivo* and prompt us to consider new interpretations to the mechanisms underlying the effects of TNF inhibitors in the treatment of inflammatory diseases. Our work also paves the way to studies focused on new arginase-1-dependent therapeutic target, such as tmTNF agonists.

Limitations of the study

Although we did not see any significant differences between WT and 3TG mice in immune cell populations in the spleen and inguinal lymph nodes and we observe an equivalent capacity of anti-TNF to interact with its ligands, we are aware that 3TG mice are just a model to study tmTNF reverse signaling and are quite different from WT mice. Indeed, WT mice express soluble TNF that participate to inflammation, and the effect of anti-TNF administration is mediated not only by tmTNF reverse signaling but also by sTNF neutralization. This lack of sTNF limits also the arthritis model that we could use. Nevertheless, we could demonstrate that tmTNF reverse signaling is a complementary mechanism of anti-inflammatory effect of anti-TNF therapies.

Resource availability

Lead contact

Information and requests for resources should be directed to and will be fulfilled by the lead contact, Dr. Rauwel Benjamin (benjamin.rauwel@inserm.fr) or Dr. Degboé Yannick (yannick.degboe@inserm.fr)

Materials availability

This study did not generate new unique reagents.

Data and code availability

All relevant data are available from the lead contact upon request.

METHODS

All methods can be found in the accompanying [Transparent methods supplemental file](#).

SUPPLEMENTAL INFORMATION

Supplemental information can be found online at <https://doi.org/10.1016/j.isci.2021.102331>.

ACKNOWLEDGMENTS

We are grateful to the flow cytometry facility of Inserm U1291 (F. L'Faqihi, and A.L. Iscache), especially V. Duplan for her help with ImageStream experiments. We thank the animal house staff members (INSERM UMS06). This work was supported by institutional grants from Inserm, Coopinter-PICS from CNRS (J.-L.D.), Région Midi-Pyrénées Occitanie R-BIO (J.-L.D.), and MSD Avenir (A. Cantagrel and J.-L.D.). K.D. received a fellowship from the Ministry of Education. N.S. benefitted from a grant issued by the "Société Française de Rhumatologie" (SFR).

AUTHOR CONTRIBUTIONS

K.D. and N.S. equally participated to this work. They carried out *in vitro* and *in vivo* experiments, analyzed data, performed statistical analyses, and revised manuscript. S.S. analyzed data and revised the manuscript, M.B. performed *in vitro* experiments and analyzed data, Y.D. performed statistical analysis, analyzed data, and revised the manuscript, J.-F.B. analyzed data and revised the manuscript, A.K. and S.N. provided tmTNF KI mice, anti-TNF MP6-XT22 antibody, and revised manuscript, and J.N. and M.A. performed *in vivo* experiments and analyzed data. N.F. analyzed data and revised manuscript, A. Constantin revised the manuscript, A. Cantagrel participated to the design of the study and revised the manuscript, and J.-L.D. conceived and designed the 3TG model, participated to the design and coordination of the study, analyzed data, and revised the manuscript. B.R. designed and supervised the project, participated to the design of 3TG model, carried out *in vitro* and *in vivo* experiments, analyzed data, performed statistical analyses, drafted and wrote the manuscript.

DECLARATION OF INTERESTS

The authors declare no competing interest.

Received: July 28, 2020

Revised: November 5, 2020

Accepted: March 16, 2021

Published: April 23, 2021

REFERENCES

- Atrekhany, K.-S.N., Nosenko, M.A., Gogoleva, V.S., Zvartsev, R.V., Qin, Z., Nedospasov, S.A., and Drutskaya, M.S. (2016). TNF neutralization results in the delay of transplantable tumor growth and reduced MDSC accumulation. *Front. Immunol.* 7, 147.
- Boyer, J.F., Balard, P., Authier, H., Faucon, B., Bernad, J., Mazieres, B., Davignon, J.L., Cantagrel, A., Pipy, B., and Constantin, A. (2007). Tumor necrosis factor alpha and adalimumab differentially regulate CD36 expression in human monocytes. *Arthritis Res. Ther.* 9, R22.
- Boyer, J.F., Baron, M., Constantin, A., Degboe, Y., Cantagrel, A., and Davignon, J.L. (2016). Anti-TNF certolizumab pegol induces antioxidant response in human monocytes via reverse signaling. *Arthritis Res. Ther.* 18, 56.
- Butler, D.M., Maini, R.N., Feldmann, M., and Brennan, F.M. (1995). Modulation of proinflammatory cytokine release in rheumatoid synovial membrane cell cultures. Comparison of monoclonal anti TNF-alpha antibody with the interleukin-1 receptor antagonist. *Eur. Cytokine Netw.* 6, 225–230.
- Cowburn, A.S., Deighton, J., Walmsley, S.R., and Chilvers, E.R. (2004). The survival effect of TNF- α in human neutrophils is mediated via NF- κ B-dependent IL-8 release. *Eur. J. Immunol.* 34, 1733–1743.
- Decoster, E., Vanhaesebroeck, B., Vandenaabeele, P., Grooten, J., and Fiers, W. (1995). Generation and biological characterization of membrane-bound, uncleavable murine tumor necrosis factor. *J. Biol. Chem.* 270, 18473–18478.
- Degboé, Y., Rauwel, B., Baron, M., Boyer, J.-F., Ruyssen-Witrand, A., Constantin, A., and Davignon, J.-L. (2019). Polarization of rheumatoid macrophages by TNF targeting through an IL-10/STAT3 mechanism. *Front. Immunol.* 10, 3.
- Deora, A., Hegde, S., Lee, J., Choi, C.H., Chang, Q., Lee, C., Eaton, L., Tang, H., Wang, D., Lee, D., et al. (2017). Transmembrane TNF-dependent uptake of anti-TNF antibodies. *MAbs* 9, 680–695.
- Eissner, G., Kirchner, S., Lindner, H., Kolch, W., Janosch, P., Grell, M., Scheurich, P., Andreesen, R., and Holler, E. (2000). Reverse signaling through transmembrane TNF confers resistance to lipopolysaccharide in human monocytes and macrophages. *J. Immunol.* 164, 6193–6198.
- Eissner, G., Kolch, W., and Scheurich, P. (2004). Ligands working as receptors: reverse signaling by members of the TNF superfamily enhance the plasticity of the immune system. *Cytokine Growth Factor Rev.* 15, 353–366.
- Feldmann, M., Williams, R.O., and Paleolog, E. (2010). What have we learnt from targeted anti-TNF therapy? *Ann. Rheum. Dis.* 69, 197–199.
- Grell, M., Douni, E., Wajant, H., Lohden, M., Claus, M., Maxeiner, B., Georgopoulos, S., Lesslauer, W., Kollias, G., Pfizenmaier, K., et al. (1995). The transmembrane form of tumor necrosis factor is the prime activating ligand of the 80 kDa tumor necrosis factor receptor. *Cell* 83, 793–802.
- Hannemann, N., Cao, S., Eriksson, D., Schnelzer, A., Jordan, J., Eberhardt, M., Schleicher, U., Rech, J., Ramming, A., Uebe, S., et al. (2019). Transcription factor Fra-1 targets arginase-1 to enhance macrophage-mediated inflammation in arthritis. *J. Clin. Invest.* 129, 2669–2684.
- Haworth, C., Brennan, F.M., Chantry, D., Turner, M., Maini, R.N., and Feldmann, M. (1991). Expression of granulocyte-macrophage colony-stimulating factor in rheumatoid arthritis: regulation by tumor necrosis factor- α . *Eur. J. Immunol.* 21, 2575–2579.
- Horiuchi, T., Mitoma, H., Harashima, S., Tsukamoto, H., and Shimoda, T. (2010). Transmembrane TNF-alpha: structure, function and interaction with anti-TNF agents. *Rheumatology (Oxford)* 49, 1215–1228.
- Ji, H., Ohmura, K., Mahmood, U., Lee, D.M., Hofhuis, F.M.A., Boackle, S.A., Takahashi, K., Holers, V.M., Walport, M., Gerard, C., et al. (2002a). Arthritis critically dependent on innate immune system players. *Immunity* 16, 157–168.

- Ji, H., Pettit, A., Ohmura, K., Ortiz-Lopez, A., Duchatelle, V., Degott, C., Gravallesse, E., Mathis, D., and Benoist, C. (2002b). Critical roles for interleukin 1 and tumor necrosis factor alpha in antibody-induced arthritis. *J. Exp. Med.* **196**, 77–85.
- Kadjani, A.A., Aghdaei, H.A., Sorrentino, D., Mirzaei, A., Shahrokhi, S., Balaii, H., Nguyen, V.Q., Mays, J.L., and Zali, M.R. (2017). Transmembrane TNF- α density, but not soluble TNF- α level, is associated with primary response to infliximab in inflammatory bowel disease. *Clin. Transl. Gastroenterol.* **8**, e117.
- Kaymakcalan, Z., Sakorafas, P., Bose, S., Scesney, S., Xiong, L., Hanzatian, D.K., Salfeld, J., and Sasso, E.H. (2009). Comparisons of affinities, avidities, and complement activation of adalimumab, infliximab, and etanercept in binding to soluble and membrane tumor necrosis factor. *Clin. Immunol.* **131**, 308–316.
- Kim, H. (2017). The transcription factor MafB promotes anti-inflammatory M2 polarization and cholesterol efflux in macrophages. *Sci. Rep.* **7**, 7591.
- Kirchner, S., Boldt, S., Kolch, W., Haffner, S., Kazak, S., Janosch, P., Holler, E., Andreesen, R., and Eissner, G. (2004). LPS resistance in monocytic cells caused by reverse signaling through transmembrane TNF (mTNF) is mediated by the MAPK/ERK pathway. *J. Leukoc. Biol.* **75**, 324–331.
- Kiswisa, L., Osorio, C., Erice, C., Vizard, T., Wyatt, S., and Davies, A.M. (2013). TNF α reverse signaling promotes sympathetic axon growth and target innervation. *Nat. Neurosci.* **16**, 865–873.
- Kitaura, H. (2005). M-CSF mediates TNF-induced inflammatory osteolysis. *J. Clin. Invest.* **115**, 3418–3427.
- Kohno, T., Tam, L.-T.T., Stevens, S.R., and Louie, J.S. (2007). Binding characteristics of tumor necrosis factor receptor-Fc fusion proteins vs anti-tumor necrosis factor mAbs. *J. Invest. Dermatol. Symp. Proc.* **12**, 5–8.
- Korganow, A.-S., Ji, H., Mangialaio, S., Duchatelle, V., Pelanda, R., Martin, T., Degott, C., Kikutani, H., Rajewsky, K., Pasquali, J.-L., et al. (1999). From systemic T cell self-reactivity to organ-specific autoimmune disease via immunoglobulins. *Immunity* **10**, 451–461.
- Kouskoff, V., Korganow, A.-S., Duchatelle, V., Degott, C., Benoist, C., and Mathis, D. (1996). Organ-specific disease provoked by systemic autoimmunity. *Cell* **87**, 811–822.
- Kratochvill, F., Neale, G., Haverkamp, J.M., Van de Velde, L.-A., Smith, A.M., Kawauchi, D., McEvoy, J., Roussel, M.F., Dyer, M.A., Qualls, J.E., et al. (2015). TNF counterbalances the emergence of M2 tumor macrophages. *Cell Rep.* **12**, 1902–1914.
- Kroner, A., Greenhalgh, A.D., Zarruk, J.G., Passos dos Santos, R., Gaestel, M., and David, S. (2014). TNF and increased intracellular iron alter macrophage polarization to a detrimental M1 phenotype in the injured spinal cord. *Neuron* **83**, 1098–1116.
- Meusch, U., Rossol, M., Baerwald, C., Hauschildt, S., and Wagner, U. (2009). Outside-to-inside signaling through transmembrane tumor necrosis factor reverses pathologic interleukin-1 β production and deficient apoptosis of rheumatoid arthritis monocytes. *Arthritis Rheum.* **60**, 2612–2621.
- Meusch, U., Klingner, M., Baerwald, C., Rossol, M., and Wagner, U. (2013). Deficient spontaneous in vitro apoptosis and increased tmTNF reverse signaling-induced apoptosis of monocytes predict suboptimal therapeutic response of rheumatoid arthritis to TNF inhibition. *Arthritis Res. Ther.* **15**, R219.
- Meusch, U., Krasselt, M., Rossol, M., Baerwald, C., Klingner, M., and Wagner, U. (2015). In vitro response pattern of monocytes after tmTNF reverse signaling predicts response to anti-TNF therapy in rheumatoid arthritis. *J. Transl. Med.* **13**, 256.
- Mitoma, H., Horiuchi, T., Hatta, N., Tsukamoto, H., Harashima, S., Kikuchi, Y., Otsuka, J., Okamura, S., Fujita, S., and Harada, M. (2005). Infliximab induces potent anti-inflammatory responses by outside-to-inside signals through transmembrane TNF- α . *Gastroenterology* **128**, 376–392.
- Mitoma, H., Horiuchi, T., Tsukamoto, H., and Ueda, N. (2018). Molecular mechanisms of action of anti-TNF- α agents – comparison among therapeutic TNF- α antagonists. *Cytokine* **101**, 56–63.
- Moss, M.L., Jin, S.-L.C., Milla, M.E., Burkhart, W., Carter, H.L., Chen, W.-J., Clay, W.C., Didsbury, J.R., Hassler, D., Hoffmann, C.R., et al. (1997). Cloning of a disintegrin metalloproteinase that processes precursor tumour-necrosis factor- α . *Nature* **385**, 733–736.
- Nesbitt, A., Fossati, G., Bergin, M., Stephens, P., Stephens, S., Foulkes, R., Brown, D., Robinson, M., and Bourne, T. (2007). Mechanism of action of certolizumab pegol (CDP870): in vitro comparison with other anti-tumor necrosis factor α agents. *Inflamm. Bowel Dis.* **13**, 1323–1332.
- Nguyen, D.X., Cotton, A., Attipoe, L., Ciurtin, C., Doré, C.J., and Ehrenstein, M.R. (2018). Regulatory T cells as a biomarker for response to adalimumab in rheumatoid arthritis. *J. Allergy Clin. Immunol.* **142**, 978–980.e9.
- Ogura, T., Tanaka, Y., and Toyoda, H. (2016). Whole cell-based surface plasmon resonance measurement to assess binding of anti-TNF agents to transmembrane target. *Anal. Biochem.* **508**, 73–77.
- Pallai, A., Kiss, B., Vereb, G., Armaka, M., Kollias, G., Szekanez, Z., and Szondy, Z. (2016). Transmembrane TNF- α reverse signaling inhibits lipopolysaccharide-induced proinflammatory cytokine formation in macrophages by inducing TGF- β : therapeutic implications. *J. Immunol.* **196**, 1146–1157.
- Ruuls, S.R., Hoek, R.M., Ngo, V.N., McNeil, T., Lucian, L.A., Janatpour, M.J., Korner, H., Scheerens, H., Hessel, E.M., Cyster, J.G., et al. (2001). Membrane-bound TNF supports secondary lymphoid organ structure but is subservient to secreted TNF in driving autoimmune inflammation. *Immunity* **15**, 533–543.
- Sabat, R., Grütz, G., Warszawska, K., Kirsch, S., Witte, E., Wolk, K., and Geginat, J. (2010). Biology of interleukin-10. *Cytokine Growth Factor Rev.* **21**, 331–344.
- Scallon, B., Cai, A., Solowski, N., Rosenberg, A., Song, X.-Y., Shealy, D., and Wagner, C. (2002). Binding and functional comparisons of two types of tumor necrosis factor Antagonists. *J. Pharmacol. Exp. Ther.* **301**, 418–426.
- Schleicher, U., Paduch, K., Debus, A., Obermeyer, S., König, T., Kling, J.C., Ribechini, E., Dudziak, D., Mouggiakakos, D., Murray, P.J., et al. (2016). TNF-mediated restriction of arginase 1 expression in myeloid cells triggers type 2 NO synthase activity at the site of infection. *Cell Rep.* **15**, 1062–1075.
- Siouti, E., and Andreaskos, E. (2019). The many facets of macrophages in rheumatoid arthritis. *Biochem. Pharmacol.* **165**, 152–169.
- Smolen, J.S., Aletaha, D., and McInnes, I.B. (2016). Rheumatoid arthritis. *Lancet* **388**, 2023–2038.
- Steggerda, S.M., Bennett, M.K., Chen, J., Emberley, E., Huang, T., Janes, J.R., Li, W., MacKinnon, A.L., Makkouk, A., Marguier, G., et al. (2017). Inhibition of arginase by CB-1158 blocks myeloid cell-mediated immune suppression in the tumor microenvironment. *J. Immunother. Cancer* **5**, 101.
- Szondy, Z., and Pallai, A. (2017). Transmembrane TNF- α reverse signaling leading to TGF- β production is selectively activated by TNF targeting molecules: therapeutic implications. *Pharmacol. Res.* **115**, 124–132.
- Tak, P.P. (2000). Analysis of synovial biopsy samples: opportunities and challenges. *Ann. Rheum. Dis.* **59**, 929–930.
- Taylor, P.C., and Feldmann, M. (2009). Anti-TNF biologic agents: still the therapy of choice for rheumatoid arthritis. *Nat. Rev. Rheumatol.* **5**, 578–582.
- Victoratos, P., and Kollias, G. (2009). Induction of autoantibody-mediated spontaneous arthritis critically depends on follicular dendritic cells. *Immunity* **30**, 130–142.
- Wajant, H., Pfizenmaier, K., and Scheurich, P. (2003). Tumor necrosis factor signaling. *Cell Death Differ.* **10**, 45–65.
- Wipke, B.T., and Allen, P.M. (2001). Essential role of neutrophils in the initiation and progression of a murine model of rheumatoid arthritis. *J. Immunol.* **167**, 1601–1608.
- Wright, H.L., Chikura, B., Bucknall, R.C., Moots, R.J., and Edwards, S.W. (2011). Changes in expression of membrane TNF, NF- κ B activation and neutrophil apoptosis during active and resolved inflammation. *Ann. Rheum. Dis.* **70**, 537–543.
- Zheng, Y., Saftig, P., Hartmann, D., and Blobel, C. (2004). Evaluation of the contribution of different ADAMs to tumor necrosis factor α (TNF α) shedding and of the function of the TNF α ectodomain in ensuring selective stimulated shedding by the TNF α convertase (TACE/ADAM17). *J. Biol. Chem.* **279**, 42898–42906.

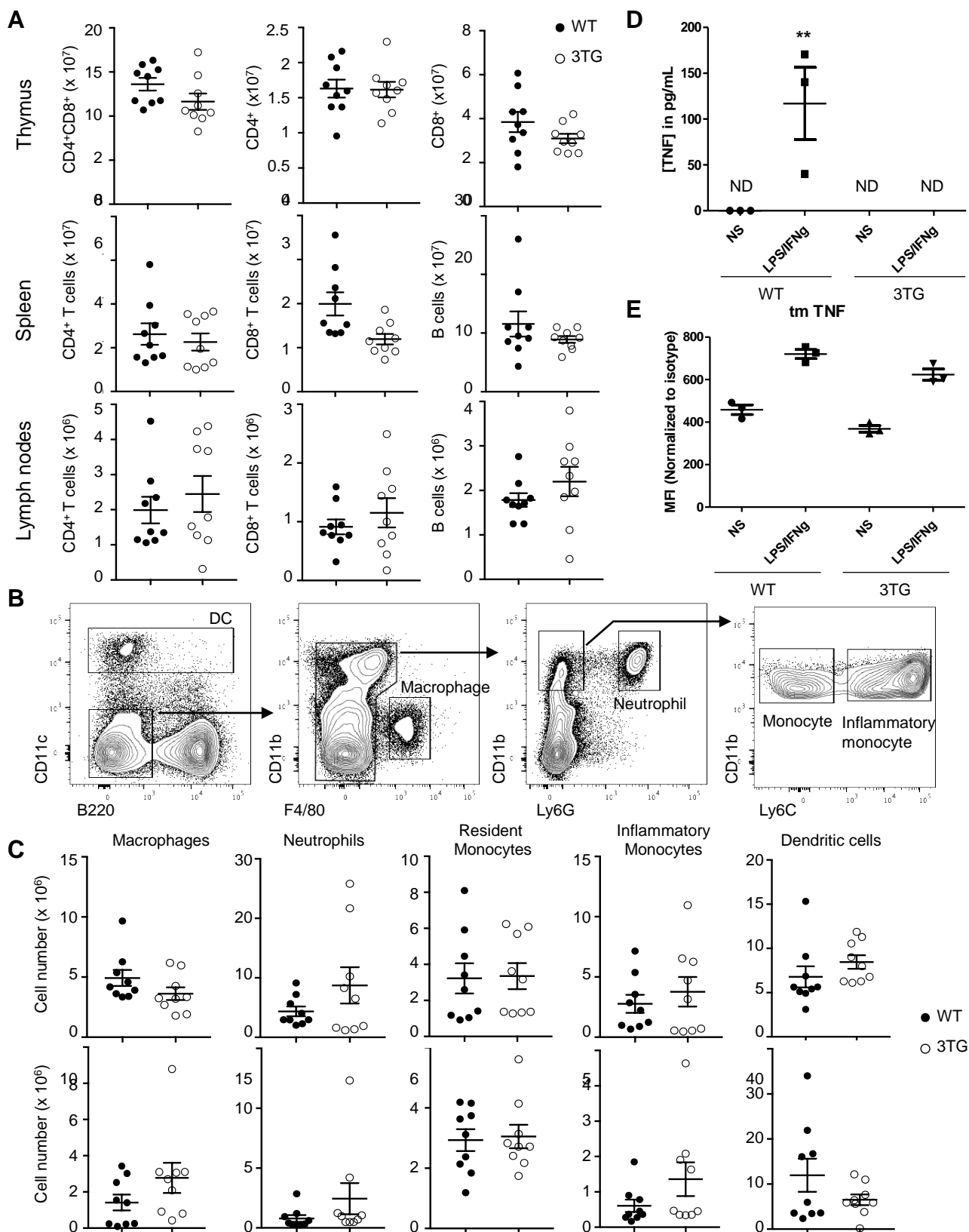
Supplemental information

Evidence for tmTNF reverse signaling *in vivo*:

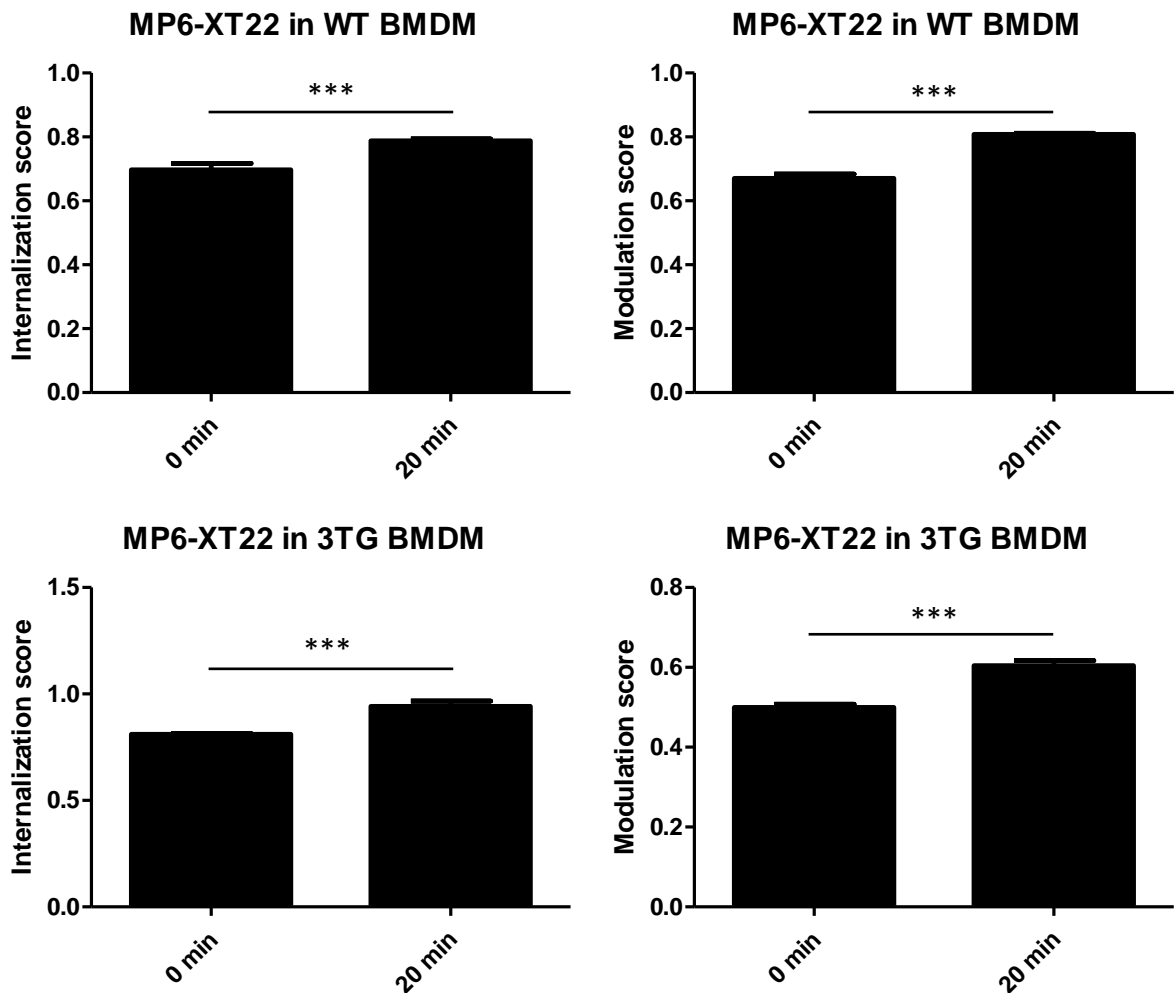
Implications for an arginase-1-mediated therapeutic

effect of TNF inhibitors during inflammation

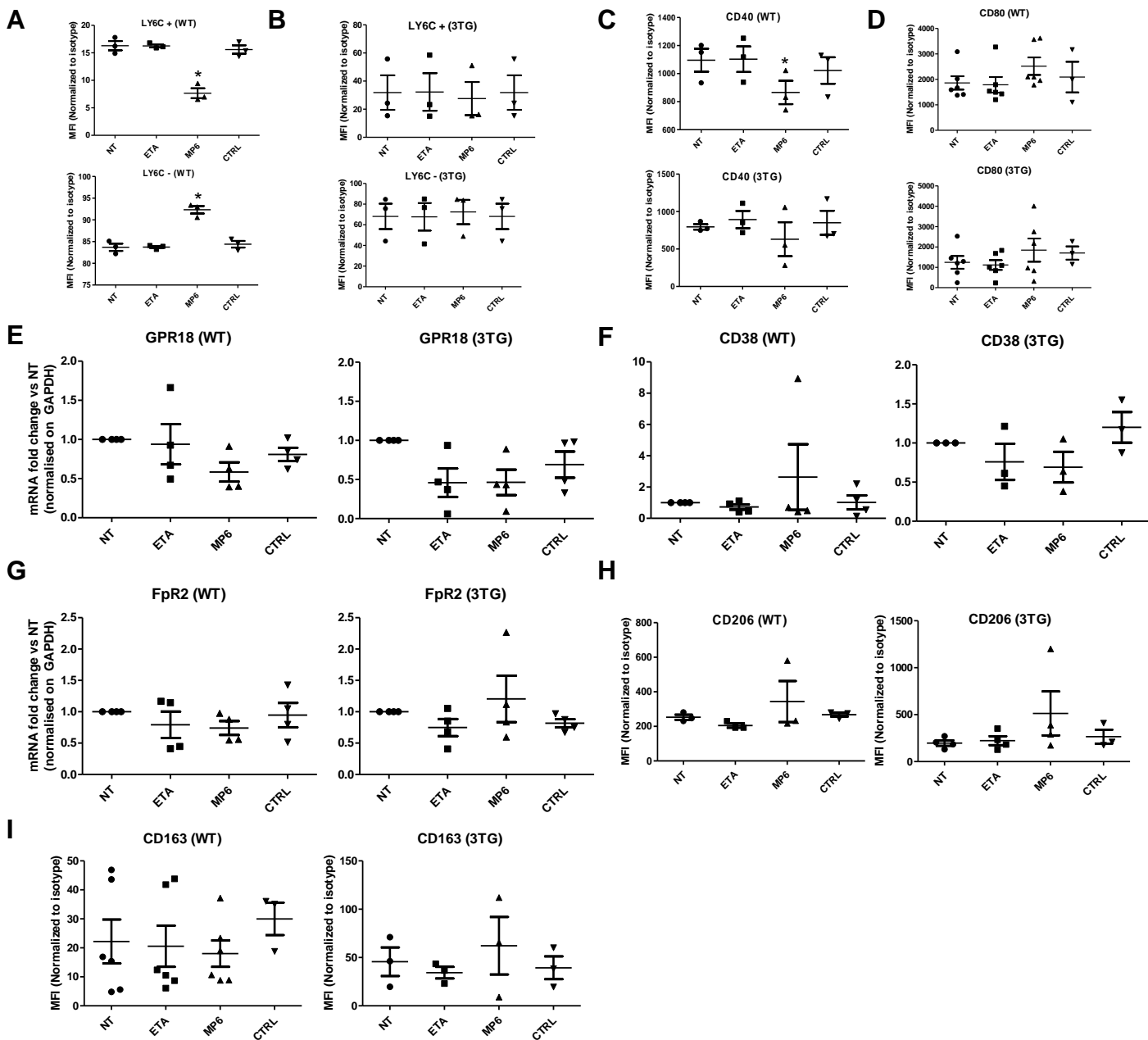
Katy Diallo, Numa Simons, Souraya Sayegh, Michel Baron, Yannick Degboé, Jean-Frédéric Boyer, Andrey Kruglov, Sergei Nedospasov, Julien Novarino, Meryem Aloulou, Nicolas Fazilleau, Arnaud Constantin, Alain Cantagrel, Jean-Luc Davignon, and Benjamin Rauwel



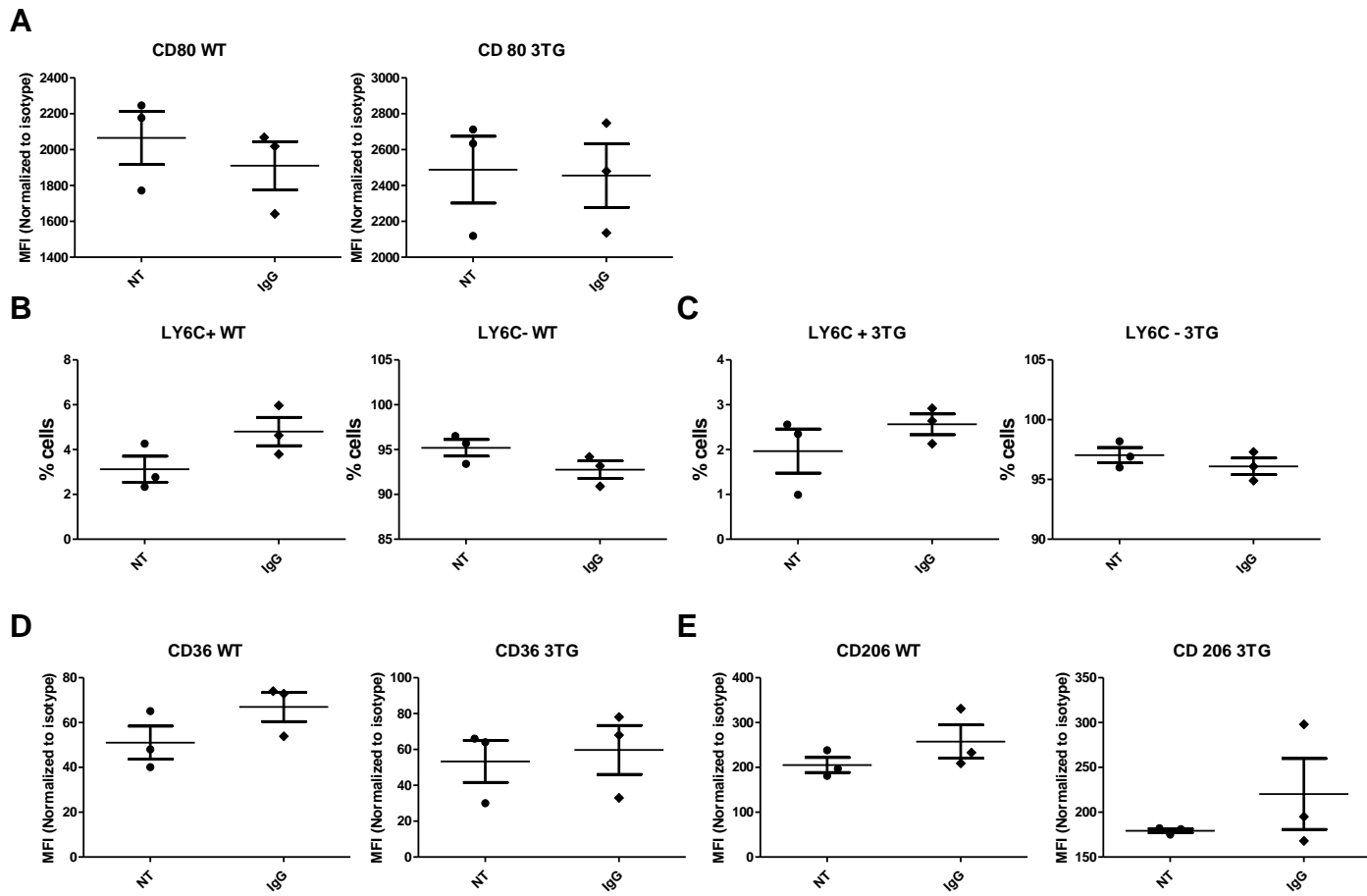
Supplementary Figure 1: Triple transgenic mouse tmTNF model invalidated for TNFR1/TNFR2, related to figure 1 to 6. (A) Cellularity of double positive CD4⁺CD8⁺, simple positive CD4⁺ and CD8⁺ thymocytes (Upper panel), cellularity of CD4⁺ T cells, CD8⁺ T cells and B cells in the spleen (middle panel) and inguinal lymph nodes (iLN) (lower panel) **(B)** Contour plots and gating strategy used for the identification of major immune cell populations in mouse spleen. Gates containing a single cell population are labeled with the included cell type **(C)** Cellularity of dendritic cells, Macrophages Neutrophils, inflammatory monocytes and resident monocytes in spleen (upper panel) and iLN (lower panel). n = 9 for each genotype. Data shown are representative from two independent experiments. Data are presented as mean \pm SEM. **(D, E)** WT and 3TG BMDM were differentiated after 7 days with recombinant M-CSF (50 ng/ml). Macrophages were then polarized into pro-inflammatory M1 macrophage during 24 hours with LPS (100 ng/ml) and IFN-g (25 ng/ml). Concentration of soluble TNF in supernatant was quantified by ELISA **(D)** and tmTNF surface expression by Flow cytometry analysis **(E)**. ELISA data represent mean \pm SEM of cytokine concentration in pg/mL (ND=non detectable, n=3, **p<0.01, Mann-Whitney U test). Cytometry data are presented as dot-plot with mean \pm SEM of MFI normalized to isotype (n=3, Mann-Whitney U test).



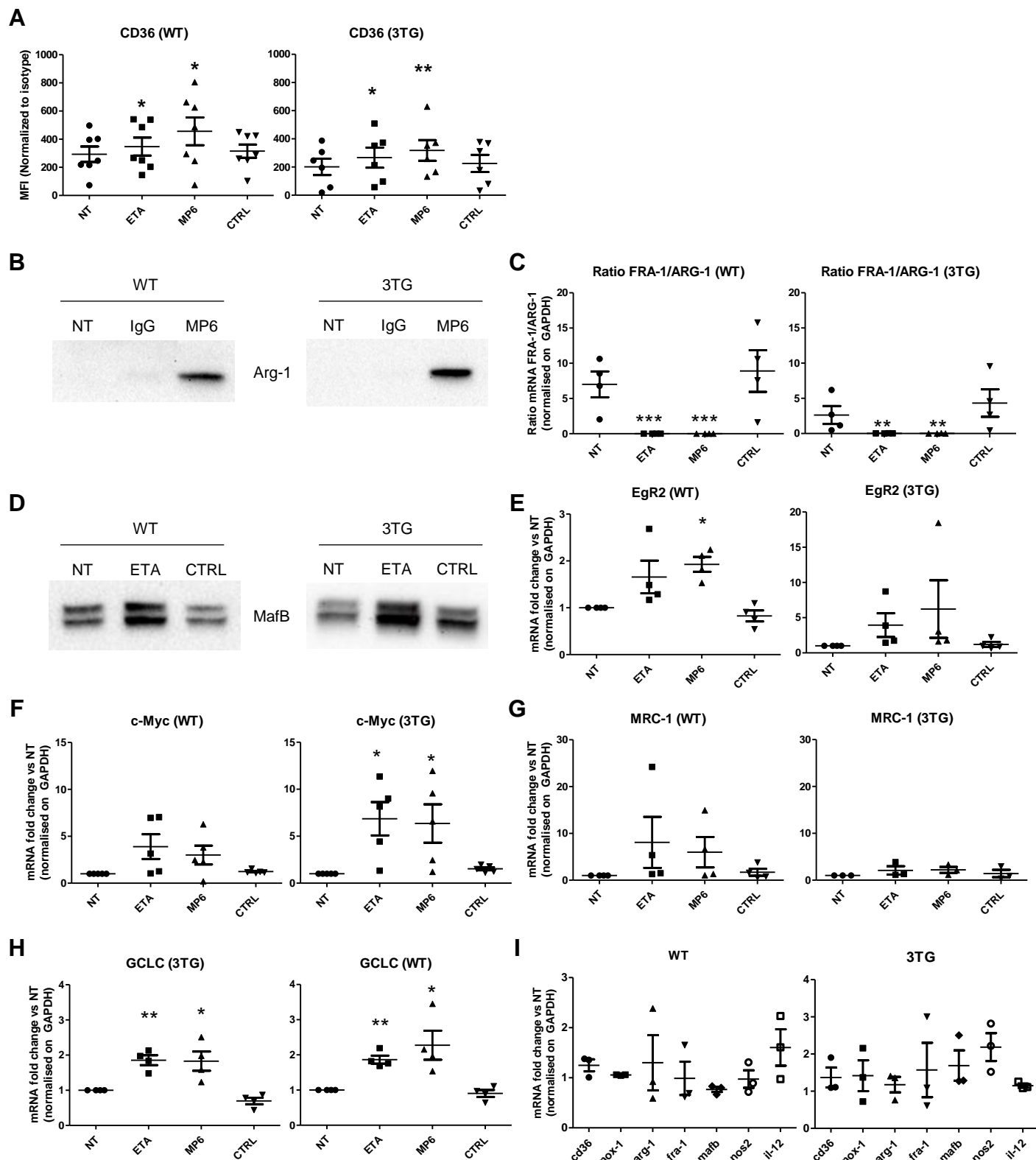
Supplementary Figure 2. Internalization of anti-TNF antibody (MP6-XT22) through its interaction with tmTNF suggests reverse signaling in macrophages, related to figure 1. Non-polarized BMDM were stimulated with LPS (50ng/mL) 30 minutes prior to staining in presence of Fc blocker with MP6-XT22-dyelight488 in WT (A) and 3TG (B) during 20 minutes at 4° (0 min) or 37°C (20min). Internalization and modulation scores were analyzed by imaging cytometry (ISX). Data are presented as mean±SEM of internalization or modulation scores (**p<0.01, ***p<0.001, n>500 events, Student's ttest). Images are representative of 3 independent experiments with more than 500 events analyzed each time.



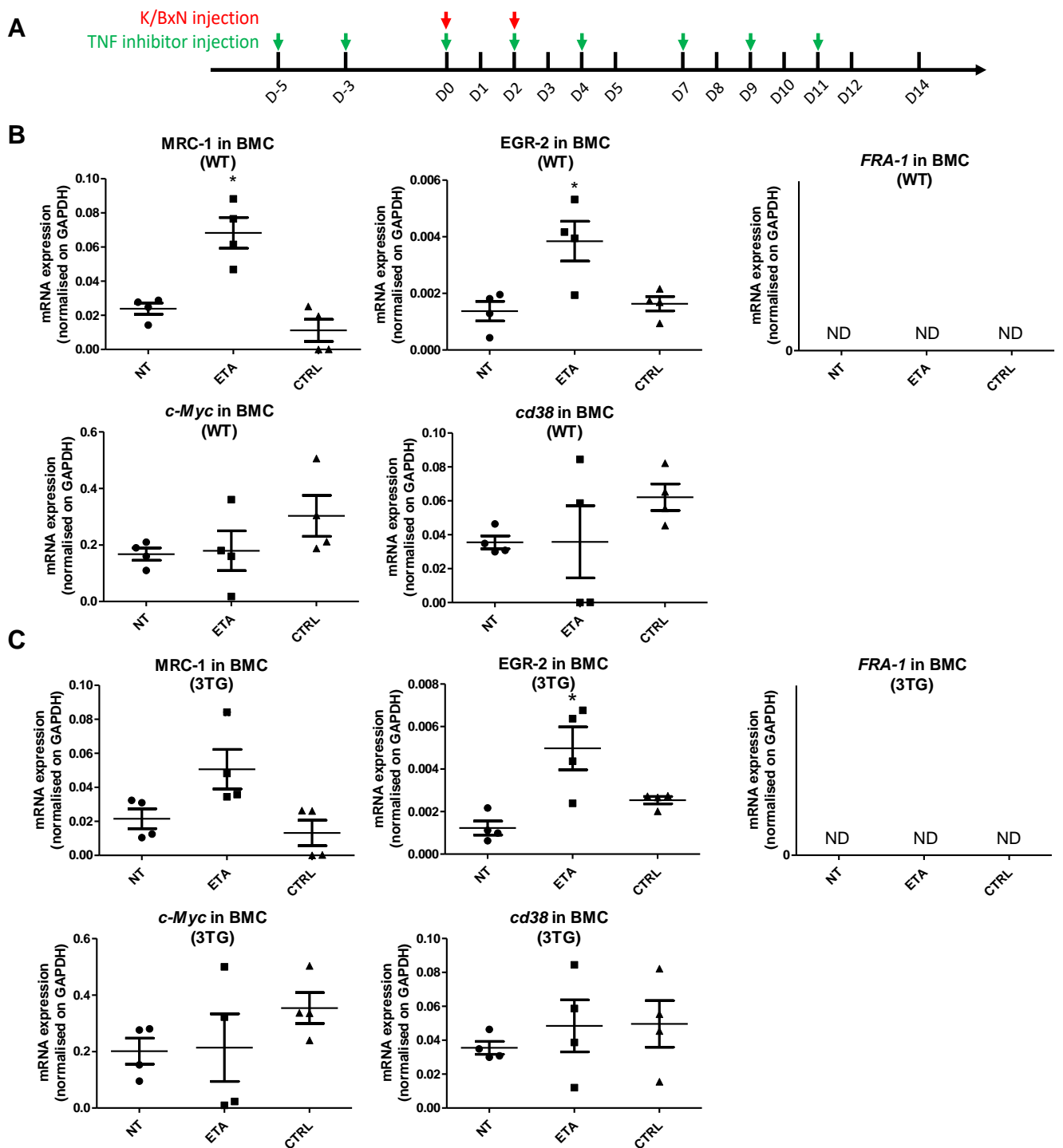
Supplementary Figure 3. Effect of tmTNF reverse signaling on macrophage polarization in vitro, related to figure 2 and 4. WT and 3TG BMDM were differentiated—after 7 days with recombinant M-CSF (50 ng/ml) in the presence or not (NT) to 10 μ /ml etanercept (ETA), anti-TNF antibody (MP6-XT22) or IgG1 control (CTRL) or left untreated (NT). Macrophages were then polarized into pro-inflammatory M1 macrophage during 24 hours with LPS (100 ng/ml) and IFN-g (25 ng/ml) in the presence or not (NT)—of fresh ETA, MP6-XT22 or CTRL. Flow cytometry analysis were performed to assess the surface expression of pro-inflammatory (Ly6C, CD40, CD80) (**A, B, C, D**) or pro-resolutive markers (CD206, CD163) (**H, I**). Cytometry data are presented as dot-plot with mean \pm SEM of MFI normalized to isotype ($n=3$ for Ly6c, CD40, CD206, and CD163, $n=6$ for CD80 and CD163 in WT BMDM, $*p<0.05$, Mann-Whitney U test performed). RNA were extracted and pro-inflammatory (*gpr18* **E**, *cd38* **F** and *fpr2* **G**) mRNA expression was analyzed by RT-qPCR in 3TG and WT BMDM. Data are presented as mean \pm SEM of mRNA fold change vs NT normalized on *gapdh*. ($n=4$, Mann-Whitney U test).



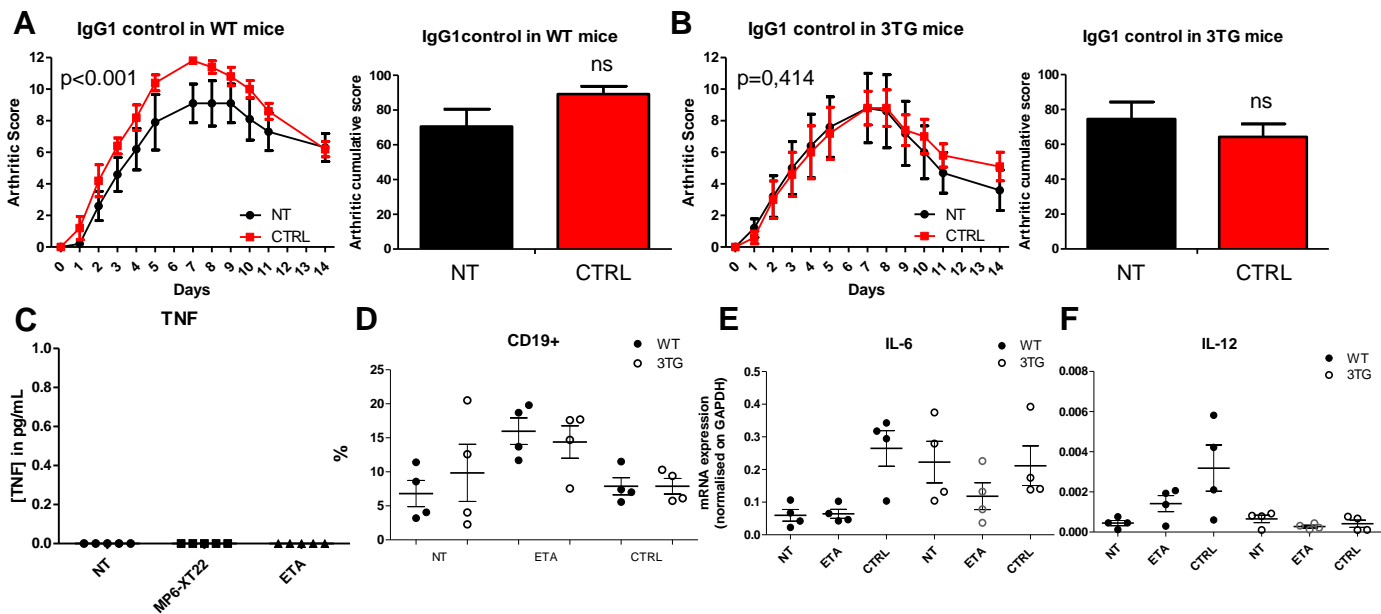
Supplementary Figure 4. Effect of tmTNF reverse signaling on macrophage polarization *in vitro*, related to figure 2 and 4. WT and 3TG BMDM were differentiated—after 7 days with recombinant M-CSF (50 ng/ml) in the presence or not (NT) to 10 μ g/ml rat IgG control (IgG). Macrophages were then polarized into pro-inflammatory M1 macrophage during 24 hours with LPS (100 ng/ml) and IFN-g (25 ng/ml) in the presence or not (NT)—of fresh IgG. Flow cytometry analysis were performed to assess the surface expression of pro-inflammatory (CD80, Ly6C) (**A, B, C**) or pro-resolutive markers (CD36, CD206) (**D, E**). Cytometry data are presented as dot-plot with mean \pm SEM of MFI normalized to isotype or % of cells for Ly6C (n=3 Mann-Whitney U test performed).



Supplementary Figure 5. Effect of tmTNF reverse signaling on macrophage polarization in vitro, related to Figure 2 and 4. WT or 3TG BMDM were obtained during 7 days of differentiation with recombinant M-CSF (50 ng/ml) in presence or absence (NT) of 10 μ g/ml of etanercept (ETA), anti-TNF antibody (MP6-XT22), human control IgG1 (CTRL) or rat control IgG (IgG, **B**, **I**) prior to being polarized into pro-inflammatory M1 macrophage during 24 hours with LPS (100 ng/ml) and IFN-g (25 ng/ml) in presence or not (NT) with fresh ETA, MP6-XT22 or CTRL. Flow cytometry analysis were performed to assess the surface expression pro-resolutive marker CD36 (**A**). Cytometry data are presented as dot-plot with mean \pm SEM of MFI normalized to isotype (n=6 in 3TG, n=7 in WT, *p<0.05, Mann-Whitney U test performed). (**B**, **C**, **D**, **E**, **F**, **G**, **H**) RNA were extracted and ratio of *fra-1/arg1* (**C**), *c-myc* (**E**), *mrc-1* (**F**) *egr-2* (**G**) and *gclc* (**H**), mRNA expression analyzed by RT-qPCR in 3TG and WT BMDM. Data are presented as mean \pm SEM of mRNA fold change vs NT normalized on *gapdh*. (n=4, *p<0.05, **p<0.01, Mann-Whitney U test performed). (**B**, **C**) Protein expression of total ARG-1 and nuclear MAFB were assessed by western-blot analysis. Results were normalized on total amount of protein with stain-free gel assay. Images are representative of 3 independent experiments. (**I**) *cd36*, *hmox-1*, *arg1*, *fra-1*, *mafb*, *iNos* and *il-12* mRNA expression analyzed. Data are presented as mean \pm SEM of mRNA fold change vs NT normalized on *gapdh*. (n=3, Mann-Whitney U test performed).



Supplementary Figure 6. In vivo arthritis experiments in WT and 3TG mice, related to Figure 5 and 6. (A) Experimental protocol of arthritis. 8-week-old 3TG or WT mice were injected at days 0 and 2 intraperitoneally with 200 μ l of 60-week-old K/BxN mice serum to induce arthritis. Mice were injected 5 and 3 days prior to inducing arthritis with 10 mg/kg of anti-TNF (ETA or MP6-XT22) or control IgG1 (CTRL) and at days 0, 2, 4, 7, 9 and 11. **(B, C)** At day 0, Bone marrow from 4 mice of each group (NT, ETA and CTRL) were collected and mRNA from precursor cells extracted. Expression of *mrc-1*, *egr-2*, *fra-1*, *c-myc* and *cd38* in WT **(B)** or 3TG **(C)** mice were analyzed by RT-qPCR. Data represent mean \pm SEM of mRNA expression normalized on *gapdh* expression (n=4). Statistics analysis were performed with Mann-Whitney U test. ND= non detectable.



Supplementary Figure 7. In vivo arthritis experiments in WT and 3TG mice, related to Figure 5 and 6. (A, B) Clinical effect of IgG1 control antibody (CTRL, 10 mg/kg) on the development of arthritis (arthritic score) in the 3TG (A) or WT (B) K/BxN serum-transferred mice (n= 5 per group). Control (NT): untreated K/BxN serum-transferred mice. Results are presented as mean arthritic score during 14 days after K/BxN injection (left panel) and arthritic cumulative score over these 14 days (right panel). Data represent mean \pm SEM. P value for arthritis score was calculated by repeated measurements two-way ANOVA test. P value for Arthritic cumulative score was calculated with Student's t-test (ns, $p > 0.05$). (C) Concentrations of TNF in blood sample of 3TG arthritic mouse were quantified by Cytometric Bead Array 7 days after K/BxN first injection. Data represent mean \pm SEM of cytokine concentration (n=5, Student's t-test). (D, E, F) Mice were sacrificed at day 7 and joints were dissected. (D) Flow cytometry analysis of % of B lymphocytes. RT-qPCR analysis of *il-6* (E) and *IL-12p40* (F) mRNA expression in WT and 3TG joints. Data represent mean \pm SEM % of leaving cells or mRNA expression normalized on GAPDH (n=4, * $p < 0.05$ as calculated with Mann-Whitney U test).

Transparent Methods

Mice

Triple transgenic mice (3TG: TNFR1^{-/-}, TNFR2^{-/-}, tmTNF^{KL/KL}) in C57BL/6 genetic background were specifically obtained by crossing existing TNFR1 and TNFR2 KO mice from Jackson laboratories to obtain TNFR1/R2 double KO that we crossed with tmTNF KI mice from our collaborators laboratory (Ruuls et al., 2001). 3TG mice were housed in a specific pathogen-free environment and cared for in accordance with European institutional guidelines (<http://eur-lex.europa.eu>). *In vivo* experiments were performed under the protocol CEEA-122 2014-62, authorized by the “Comité d'éthique en matière d'expérimentation animale CEEA122-US006/CREFRE”.

Organ and cell isolation

Single-cell suspensions were prepared by standard mechanical disruption for thymus and filtered through a nylon mesh. Spleen and inguinal lymph node (iLN) were first enzymatically digested Liberase (50ug/ml, Roche) and DNase I (10ug/ml, Roche Molecular Biochemicals) for 20 min at 37 °C. Cells were counted and surface stained with: anti-B220-PECy7 (RA3-6B2, BioLegend), anti-Ly6C-BV711 (HK1.4, Biolegend), anti-CD8-PE-CF594 (53-6.7, BD Biosciences), Anti-CD8-PE-CF594 (53-6.7, BD Biosciences), Ly6G-FITC (1A8, BD Biosciences), anti-CD11c-PE-CF594 (HL3, BD Biosciences), Streptavidin-BV605 (BD Biosciences), anti-CD3-V500 (500A2, BD Biosciences), anti-CD4-PerCP-Cyanine5.5 (RM4-5, eBioscience), anti-CD11b-PE-Cy5 (M1/70, eBioscience) and F4/80-biot (BM8, eBioscience). Cells were stained with Fixable Viability Dye eFluor506 (eBioscience, Cat#65-0866) or Dye eFluor450 (eBioscience, Cat#65-0863). Labelled cells were acquired and analyzed using an LSRII flow cytometer (BD Biosciences, San Jose, CA) and FlowJo software (Tree Star, Ashland, OR). Doublets and dead cells were excluded using appropriate FSC/SSC gates.

Bone marrow derived macrophages (BMDM)

To generate BMDM, bone marrow cells from femurs and tibias of mice were harvested using aseptic techniques. Marrow cores were flushed into sterile tubes using syringes fitted with 23 gauge needles and filled with PBS. Cells were filtrated on 100 µm nylon cell strainer and red blood cells were lysed in lysis

buffer (0.15 m NH₄Cl, 10 mm KHCO₃, and 0.1 mm Na₂EDTA, pH 7.4). Cells were washed once in PBS then plated and cultured at a density of 5-6x10⁶cells/well (6-well plate, Falcon poly-styrene) in Dulbecco's Modified Eagle Media (DMEM, Invitrogen) supplemented with 10% heat-inactivated fetal bovine serum (FBS) (Life Technologies), 1% penicillin/streptomycin (Invitrogen) and recombinant M-CSF (50 ng/mL, peprotech), in the presence or absence of 5 µg/mL of soluble TNF-R2 (Etanercept, ETA), anti-murine TNF rat antibody (MP6-XT22) or anti-human IL-17 monoclonal antibody (Secukinumab, CTRL) as a non-relevant antibody control. After 7 days of differentiation, fresh ETA, MP6-XT22 or CTRL were added to media and cells were classically polarized into macrophages M1 in the presence of LPS (100 ng/ml, Sigma-Aldrich L2880) + IFN-γ (25 ng/mL, peprotech) for 24 hours.

Arthritis model

8-weeks-old 3TG or WT male mice were injected at days 0 and 2 intraperitoneally with 200 µl of 60-week-old K/BxN mice serum to induce arthritis. Soluble TNF receptor 2 (Etanercept, ETA, Pfizer), anti-mouse TNF rat antibody (MP6-XT22) or IgG1 control antibody (CTRL, Secukinumab, Novartis Pharma) were injected intraperitoneally at 10 mg/kg, 5 and 3 days prior to the first K/BxN serum injection and at days 0, 2, 4, 7, 9 and 11. Mice were sacrificed at day 0 or 14 days after the first K/BxN injection. Each joint was examined daily for swelling and redness. Severity of arthritis in K/BxN-injected mice was assessed macroscopically in a blinded fashion for each paw per mouse with a three-grade score (Grade 0 = normal; grade 0.5 = swelling of fingers; grade 1 = light swelling of the joint and/or redness of the footpad; grade 2 = obvious swelling of the joint and grade 3 = severe swelling of the joint with redness of the footpad). A severity score was calculated for the four limbs (maximum 12 points for individual mice). Cumulative arthritis score for all mice was calculated at day 14. Swelling of the two hindpaws was measured with a digital caliper and averaged. Blood samples were collected at the peak of arthritis score, 7 days after K/BxN serum injection. Progenitor cells from bone marrow were collected at day 0 to study the effect of anti-TNF pre-injection. At day 7, mice were sacrificed and knees and ankles joints were dissected mechanically in presence of DNase and Collagenase D. Purified cells were then separated in two, one half for flow cytometry analysis and one half for RT-qPCR analysis.

Internalization assay

We used imaging cytometry to determine if soluble TNF receptor 2 (Etanercept, ETA, Pfizer) molecules bind tmTNF and are internalized into BMDM. BMDM were stimulated for 30 min with LPS (50 ng/mL) to increase tmTNF cell surface expression. Cells were then harvested, resuspended in PBS containing 5% FCS and incubated in the presence of anti-H-2 (I-A / I-E, 15-532-81, ebioscience) or ETA conjugated to PE-Cy5 or DyeLight488 respectively. H-2 was used as a non-internalized control. Staining was operated 30 min at 37°C to permit internalization. A control staining at 4°C to block internalization was performed in parallel. Cells were washed and resuspended in PBS, 5mM EDTA prior to analysis by Image Stream X Mark II (Merck Millipore). Internalization and modulation scores of tmTNF/soluble receptors were calculated through the ratio of intracellular fluorescence to Total fluorescence. Modulation score indicates the concentration of fluorescence in spots as opposed to scattered signal.

RNA extraction and RT-qPCR

BMDM were harvested and analyzed after 7 days of differentiation and 24 hours of M1 polarization. RNA was extracted by using High Pure RNA Isolation Kit (Roche, and reverse transcribed with RevertAid Reverse Transcriptase (ThermoFisher Scientific, Waltham, MA, USA) according to the manufacturer's instructions. All qPCRs were performed with SYBR green mix (Roche, Switzerland).

All RT-qPCR were performed with the following primers:

gapdh	Forward	5'-TTCACCACCATGGAGAAGG-3'
	Reverse	5'-CACACCCATCACAAACATGG-3'
ho-1	Forward	5'-GGTGATGGCTTCCTTGTACC-3'
	Reverse	5'-AGTGAGGCCCATACCAGAAG-3'
cd36	Forward	5'-TCCTCTGACATTTGCAGGTCTATC-3'
	Reverse	5'-AAAGGCATTGGCTGGAAGAA-3'

gclc	Forward	5'-GCACGGCATCCTCCAGTTCCT-3'
	Reverse	5'-TCGGATGGTTGGGGTTTGTCC-3'
cd38	Forward	5'-TCAGCCACTAATGAAGTTGGGA-3'
	Reverse	5'-CTGGACCTGTGTGAACTGATGG-3'
gpr18	Forward	5'-GACAGACAGGAGGTTTCGACATACA-3'
	Reverse	5'-ACCGAGGTGTGGGTCTCCTTATGT-3'
fpr2	Forward	5'-CTGAATGGATCAGAAGTGGTGG-3'
	Reverse	5'-CCCAAATCACTAGTCCATTGCC-3'
egr-2	Forward	5'-GCCAAGGCCGTAGACAAAATC-3'
	Reverse	5'-CCACTCCGTTTCATCTGGTCA-3'
c-myc	Forward	5'-CGGACACACAACGTCTTGGAA-3'
	Reverse	5'-AGGATGTAGGCGGTGGCTTTT-3'
il-6	Forward	5'-TACCCCAATTTCCAATGCTC-3'
	Reverse	5'-TCTTGGTCCTTAGCCACTCC-3'
arg1	Forward	5'-GAATCTGCATGGGCAACC-3'
	Reverse	5'-GAATCCTGGTACATCTGGGAAC-3'
il-10	Forward	5'-CAGAGCCACATGCTCCTAGA-3'
	Reverse	5'-TGTCCAGCTGGTCCTTTGTT-3'
il-12	Forward	5'-TTGCTGGTGTCTCCACTCAT-3'
	Reverse	5'-GGGAGTCCAGTCCACCTCTA-3'
mrc1	Forward	5'-CCACAGCATTGAGGAGTTTG-3'

	Reverse	5'-ACAGCTCATCATTTGGCTCA-3'
nos2	Forward	5'-CCGGAGCCTTTAGACCTCA-3'
	Reverse	5'-TTCAGCCTCATGGTAAACACA-3'
fra-1	Forward	5'-CCCAGTACAGTCCCCCTCA-3'
	Reverse	5'-TCCTCCTCTGGGCTGATCT-3'
il-1 β	Forward	5'-TGAAAGACGGCACACCCA-3'
	Reverse	5'-AAACCGCTTTTCCATCTTCTTCT-3'

Western Blot Analysis

Cell lysates were subjected to SDS/PAGE on 4–15% Mini-Protean TGX Stain-Free Gels (BioRad, Hercules, CA, USA). After transferring on 0.22 μ m nitrocellulose membrane, proteins were revealed using specific antibodies (MafB rabbit monoclonal antibody, clone BLR046F, Bethyl laboratories, Montgomery, TX, USA) and anti-rabbit HRP-linked polyclonal antibodies (Cell Signaling, Danvers, MA, USA). Protein expression was normalized on total protein amount using stain-free technology following manufacturer's instructions.

Flow cytometry

Evaluation of the effect of reverse signaling on M1 polarization of BMDM was assessed by studying the expression of surface markers by flow cytometry. The cells were stimulated for 24 hours with 100 ng/ml lipopolysaccharide (LPS) and 25 ng/ml interferon γ (IFN γ). For extracellular labeling, non-specific Ab binding was blocked with addition of blocking buffer PBS 20% SVF. Cells were washed prior to being labeled with antibodies described in supplemental materials. F4 / 80 FITC (clone BM8, Biolegend), CD36 PE (ME542 clone, Santa Cruz Biotechnology), CD206 (clone C068C2, Biolegend), CD163 PE (clone TNKUPJ, Invitrogen), CD80 FITC (clone 16-10A1, Biolegend), Ly6C PE (clone AL21, BD Biosciences). Flow cytometry was performed by using a MACSQuant analyzer 10 (Miltenyi) and data were analyzed using FlowJo software.

Cytokine concentration analysis

IL-6, IL-10, TNF and IL12p70 concentrations in blood samples and 24h M1 polarized BMDM supernatants were analyzed by Cytometric Bead Array (CBA, BD Biosciences) according to manufacturer's instructions. Data was acquired on an LSRII cytometer (BD Biosciences) and analyzed using FCAP Array v3 software (BD Biosciences). 24 hours secretion kinetic of IL-1 β , TNF and IL-10 in M1 polarized BMDM were analyzed by ELISA (Biolegend).

Statistical analysis

All data were analyzed with GraphPad Prism5. Normality was tested by Agostino and Pearson test. *In vitro* data were analyzed with Student's T-test or Mann-Whitney U-test. *In vivo* arthritis experiments data were analyzed with repeated-measurements two-way ANOVA test. Data are represented as mean \pm SEM, and $p < 0.05$ (two-tailed) was considered to be statistically significant.